

Cosmological Perturbation Theory in the Synchronous and Conformal Newtonian Gauges

Chung-Pei Ma¹

Theoretical Astrophysics 130-33, California Institute of Technology, Pasadena, CA 91125
and

Edmund Bertschinger²

Department of Physics, Massachusetts Institute of Technology, Cambridge, MA 02139

ABSTRACT

This paper presents a systematic treatment of the linear theory of scalar gravitational perturbations in the synchronous gauge and the conformal Newtonian (or longitudinal) gauge. It differs from others in the literature in that we give, in both gauges, a complete discussion of all particle species that are relevant to any flat cold dark matter (CDM), hot dark matter (HDM), or CDM+HDM models (including a possible cosmological constant). The particles considered include CDM, baryons, photons, massless neutrinos, and massive neutrinos (an HDM candidate), where the CDM and baryons are treated as fluids while a detailed phase-space description is given to the photons and neutrinos. Particular care is applied to the massive neutrino component, which has been either ignored or approximated crudely in previous works. Isentropic initial conditions on super-horizon scales are derived. The coupled, linearized Boltzmann, Einstein and fluid equations that govern the evolution of the metric and density perturbations are then solved numerically in both gauges for the standard CDM model and two CDM+HDM models with neutrino mass densities $\Omega_\nu = 0.2$ and 0.3 , assuming a scale-invariant, adiabatic spectrum of primordial fluctuations. We also give the full details of the cosmic microwave background anisotropy, and present the first accurate calculations of the angular power spectra in the two CDM+HDM models including photon polarization, higher neutrino multipole moments, and helium recombination. The numerical programs for both gauges are available at <http://arcturus.mit.edu/cosmics>.

Subject headings: cosmic microwave background — cosmology: theory — large-scale structure of universe — gravitation

¹e-mail: cpma@daffy.tapir.caltech.edu

²e-mail: bertschinger@mit.edu

1. Introduction

The theory of galaxy formation based on gravitational instability is aimed at describing how primordially-generated fluctuations in matter and radiation grow into galaxies and clusters of galaxies due to self-gravity. A perturbation theory can be formulated when the amplitudes of the fluctuations are small, and the growth of the fluctuations can be solved from the linear theory.

In the early universe, gravitational perturbations are inflated to wavelengths beyond the horizon at the end of the inflationary epoch. Fluctuations of a given length scale reenter the horizon at a later time when the horizon has grown to the size of the fluctuations. Although the process of galaxy formation in recent epochs is well described by Newtonian gravity (and other physical processes such as hydrodynamics), a general relativistic treatment is required for perturbations on scales larger than the horizon size before the horizon crossing time. The use of general relativity brought in the issue of gauge freedom which has caused some confusion over the years. Lifshitz (1946) adopted the “synchronous gauge” for his coordinate system, which has since become the most commonly used gauge for cosmological perturbation theories. However, some complications associated with this gauge such as the appearance of coordinate singularities and spurious gauge modes prompted Bardeen (1980) and others (e.g. Kodama & Sasaki, 1984) to formulate alternative approaches that deal only with gauge-invariant quantities. A thorough review of the gauge-invariant perturbation theory and its application to texture-seeded structure formation models is given by Durrer (1993). Another possibility is to adopt a different gauge. We will discuss in detail in this paper the conformal Newtonian (or the longitudinal) gauge (Mukhanov, Feldman & Brandenberger 1992), which is a particularly convenient gauge to use for scalar perturbations. It also has the feature that the two scalar fields that describe the metric perturbations in this gauge are identical (up to a minus sign) to the gauge-invariant variables Bardeen (1980) constructed.

The linear theory for a perturbed Friedmann-Robertson-Walker universe was first developed by Lifshitz (1946), later reviewed in Lifshitz & Khalatnikov (1963). The subsequent work can be found summarized in the textbooks by Weinberg (1972) and Peebles (1980), in the reviews by Kodama & Sasaki (1984) and Mukhanov et al (1992), and in the Summer School lectures by Efstathiou (1990), Bertschinger (1995), and Bond (1995). The theory has been applied to various cosmological models. In the synchronous gauge, for example, Peebles & Yu (1970) solved the linear evolution equations for photons and baryons in the absence of massless neutrinos and non-baryonic dark matter. Bond and Szalay (1983) included the neutrinos but approximated them as a perfect fluid by using only the first two moments in the angular expansion of the neutrino distribution function. They also did not include CDM. Xiang & Kiang (1992) considered both CDM and massive neutrinos, but treated the latter as non-relativistic particles and also ignored massless neutrinos. Holtzman (1989) provided fitting formulas for the baryonic transfer functions in various cosmological models, but gave no detailed description of the calculation, and again included only the first two moments of the neutrino distribution function. Durrer (1989) obtained

numerical solutions for the perturbations in the gauge-invariant formalism in the absence of baryons. Instead of using the convenient multipole expansion technique, Stompor (1994) adopted the earliest method by solving the massive neutrino distribution function directly at discrete momenta and angles.

Another important application of the linear theory is to the cosmic microwave background anisotropies. The early calculations of the radiation perturbations included only the baryons and the photons (Peebles & Yu 1970; Wilson & Silk 1981). The calculations were subsequently extended to dark matter dominated models (e.g. Bond & Efstathiou 1984, 1987; Vittorio & Silk 1984, 1992; Holtzman 1989). The post-COBE era has seen a rapid increase in the number of papers on this subject (see Sugiyama & Gouda 1992; White, Scott, & Silk 1994; and references therein). However, there has not been a complete treatment of the massive neutrinos to the accuracy that is needed for comparison with the near-future anisotropy experiments. Truncating the *massless* neutrino moments beyond $l \geq 2$ in the pure CDM model leads to a 10% error in the anisotropy power spectrum (Hu et al 1995). One would expect a comparable or larger error if the $l \geq 2$ modes were not included for the massless *and* massive neutrinos in CDM+HDM models.

This paper differs from earlier ones in the literature in that we give a complete discussion of all particle species that are relevant to any flat CDM, HDM, or CDM+HDM models (including a possible cosmological constant). These include CDM, baryons, photons, massless neutrinos, and massive neutrinos (an HDM candidate). The recent interests in CDM+HDM models (e.g. Davis, Summers, & Schlegel 1992; Klypin et al 1993; Jing et al 1994; Cen & Ostriker 1994; Ma & Bertschinger 1994b; Ma 1994; Primack et al 1995; Klypin et al 1995) prompted us to provide a detailed treatment of the massive neutrino component, which was either ignored or crudely approximated in other works. Part of the cause for neglecting this component was perhaps a lack of motivation when the standard CDM model was thought to match the observed structure well. Another was perhaps due the sharp increase in the computing time required to deal with the time-dependent nature of the massive neutrinos' energy-momentum relation. For completeness, we also give full details and results of the calculation of the cosmic microwave background anisotropy including photon polarization and helium recombination.

This paper serves two purposes. First, it is an independent paper in which we present a systematic treatment of the linear theory of scalar isentropic gravitational perturbations in the synchronous and conformal Newtonian gauges. The coupled, linearized Einstein, Boltzmann, and fluid equations for the metric and density perturbations are presented in parallel in the two gauges. The CDM and the baryon components behave like collisionless and collisional fluids, respectively, while the photons and the neutrinos require a phase-space description governed by the Boltzmann transport equation. We also derive analytically the time dependence of the perturbations on scales larger than the horizon to illustrate the dependence on the gauge choice. This information is needed in the initial conditions for the numerical integration of the evolution equations.

This paper also serves as a companion paper to Ma & Bertschinger (1994a) in which we

reported the main results from our linear calculation of the full neutrino phase space in a CDM+HDM model with $\Omega_c = 0.65$, $\Omega_\nu = 0.3$, $\Omega_{\text{baryon}} = 0.05$, and $H_0 = 50 \text{ km s}^{-1} \text{ Mpc}^{-1}$. (The corresponding neutrino mass is $m_\nu = 7 \text{ eV}$.) The motivation was to obtain an accurate sampling of the neutrino phase space for the HDM initial conditions in subsequent N -body simulations (Ma & Bertschinger 1994b; Ma 1994) of structure formation in CDM+HDM models. We adopted a two-step Monte Carlo procedure to achieve this goal: (1) Integrate the coupled, linearized Boltzmann, Einstein, and fluid equations for all particle species in the model (i.e., CDM, HDM, photons, baryons and massless neutrinos) to obtain the evolution of the metric perturbations; (2) Follow the trajectories of individual neutrinos by integrating the geodesic equations using the metric computed in (1). Since no coordinate singularities occur in the conformal Newtonian gauge and the geodesic equations have simple forms, the geodesic integration in step (2) was carried out in this gauge, starting shortly after neutrino decoupling at redshift $z \sim 10^9$ until $z = 13.5$. We focus on step (1) in this paper. Following historical precedents, we first developed the code for the Boltzmann integration in the synchronous gauge. The transformation relating the synchronous gauge and the conformal Newtonian gauge was then derived and used to compute the metric perturbations in the latter gauge for step (2) of the calculation. Subsequently we developed a code to perform the full integration in the conformal Newtonian gauge.

The organization of this paper is as follows. In §2 we write down the metric for the two gauges and summarize their properties. In §3, we derive the gauge transformation relating two arbitrary gauges and obtain the transformation between the synchronous and the conformal Newtonian gauges. The linearized evolution equations for the metric and the density perturbations are given in §§4 and 5. Section 4 discusses the Einstein equations with emphasis on the source terms, the energy-momentum tensor, in the two gauges. The perturbed fluid equations are derived from the energy-momentum conservation, which are applied to CDM and the baryons in §5. The rest of §5 contains detailed treatments of the photon and neutrino phase space distributions, recombination, and the coupling of photons and baryons. The photon and neutrino distribution functions are expanded in Legendre polynomials, reducing the linearized Boltzmann equation to a set of coupled ordinary differential equations for the expansion modes. The massive neutrinos require a slightly more complicated treatment because the energy-momentum relation depends nontrivially on time when the neutrinos make a transition from being relativistic to non-relativistic. Our method for computing the microwave background anisotropy is presented in §6. Section 7 discusses the behavior of the perturbations before horizon crossing. The necessary initial conditions for the variables in the two gauges are given. Section 8 presents the numerical results for the evolution of the perturbations and the angular power spectrum of the microwave anisotropy in CDM+HDM models.

The complex physics we study requires the use of many equations and symbols. As a guide to the reader, in Table 1 we summarize the key symbols and the equations where they are defined or first used.

Symbol	Meaning	Reference Eqn
a	scale factor	(1)
τ	conformal time	(1)
k	wavenumber of Fourier mode	(4)
P_i	conjugate momentum to (comoving) position x^i	(31)
p_i	proper momentum	(31)
q_i	$= ap_i$	–
ϵ	$= (q^2 + a^2 m^2)^{1/2}$	–
h	synchronous	(1), (4)
η	metric perturbations	
ϕ	conformal Newtonian	(5)
ψ	metric perturbations	
subscript c	cold dark matter	–
subscript ν	massless neutrinos	–
subscript h	massive neutrinos	–
subscript γ	photons	–
subscript b	baryons	–
f_0	unperturbed phase space distribution function	(33)
Ψ	perturbation to f_0	(35)
Ψ_l	l th Legendre component of Ψ	(54)
F_l	momentum-averaged Ψ_l	(46)
$G_{\gamma l}$	photon polarization component	(62)
δ	density fluctuation ($= F_0$)	(27a), (47)
θ	divergence of fluid velocity ($= 3kF_1/4$)	(22), (27b), (47)
σ	shear stress ($= F_2/2$)	(22), (27d), (47)
Δ	temperature fluctuation ($= \Delta T/T = F_\gamma/4$)	(82)
Δ_l	l th Legendre mode of Δ ($= F_{\gamma l}/4$)	(84)
C_l	temperature fluctuation power spectrum	(87)
c_s	baryon sound speed ($= \delta P_b/\delta \rho_b$)	(68)
c_{pb}	sound speed of coupled photon-baryon fluid	(99)
w	describes equation of state ($= P/\rho$)	(29),(30)
n_e	electron number density	(59)
σ_T	Thomson scattering cross section	(59)
τ_c	$= (an_e \sigma_T)^{-1}$	(71)
R_ν	density ratio $\bar{\rho}_\nu/(\bar{\rho}_\gamma + \bar{\rho}_\nu)$	(92)
R	density ratio $(4/3)\bar{\rho}_\gamma/\bar{\rho}_b$	(70)

Table 1: Symbols used in this paper.

2. The Two Gauges

We consider only spatially flat ($\Omega = 1$) background spacetimes with isentropic scalar metric perturbations. The spacetime coordinates are denoted by x^μ , $\mu \in (0, 1, 2, 3)$, where x^0 is the time component and x^i , $i \in (1, 2, 3)$ are the spatial components in Cartesian coordinates. Greek letters α, β, γ and so on always run from 0 to 3, labeling the four spacetime-coordinates; Roman letters such as i, j, k always run from 1 to 3, labeling the spatial parts of a four-vector. Repeated indices are summed. Since our interests lie in the physics in an expanding universe, we use comoving coordinates $x^\mu = (\tau, \vec{x})$ with the expansion factor $a(\tau)$ of the universe factored out. The comoving coordinates are related to the proper time and positions t and \vec{r} by $dx^0 = d\tau = dt/a(\tau)$, $d\vec{x} = d\vec{r}/a(\tau)$. Dots will denote derivatives with respect to τ : $\dot{a} \equiv \partial a / \partial \tau$. The speed of light c is set to unity.

The components g_{00} and g_{0i} of the metric tensor in the synchronous gauge are by definition unperturbed. The line element is given by

$$ds^2 = a^2(\tau) \{-d\tau^2 + (\delta_{ij} + h_{ij})dx^i dx^j\}. \quad (1)$$

The metric perturbation h_{ij} can be decomposed into a trace part $h \equiv h_{ii}$ and a traceless part consisting of three pieces, h_{ij}^{\parallel} , h_{ij}^{\perp} , and h_{ij}^T , where $h_{ij} = h\delta_{ij}/3 + h_{ij}^{\parallel} + h_{ij}^{\perp} + h_{ij}^T$. By definition, the divergences of h_{ij}^{\parallel} and h_{ij}^{\perp} (which are vectors) are longitudinal and transverse, respectively, and h_{ij}^T is transverse, satisfying

$$\epsilon_{ijk} \partial_j \partial_l h_{lk}^{\parallel} = 0, \quad \partial_i \partial_j h_{ij}^{\perp} = 0, \quad \partial_i h_{ij}^T = 0. \quad (2)$$

It then follows that h_{ij}^{\parallel} can be written in terms of some scalar field μ and h_{ij}^{\perp} in terms of some divergenceless vector \vec{A} as

$$\begin{aligned} h_{ij}^{\parallel} &= \left(\partial_i \partial_j - \frac{1}{3} \delta_{ij} \nabla^2 \right) \mu, \\ h_{ij}^{\perp} &= \partial_i A_j + \partial_j A_i, \quad \partial_i A_i = 0. \end{aligned} \quad (3)$$

The two scalar fields h and μ (or h_{ij}^{\parallel}) characterize the scalar mode of the metric perturbations, while A_i (or h_{ij}^{\perp}) and h_{ij}^T represent the vector and the tensor modes, respectively.

We will be working in the Fourier space k in this paper. We introduce two fields $h(\vec{k}, \tau)$ and $\eta(\vec{k}, \tau)$ in k -space and write the scalar mode of h_{ij} as a Fourier integral

$$h_{ij}(\vec{x}, \tau) = \int d^3 k e^{i\vec{k} \cdot \vec{x}} \left\{ \hat{k}_i \hat{k}_j h(\vec{k}, \tau) + \left(\hat{k}_i \hat{k}_j - \frac{1}{3} \delta_{ij} \right) 6\eta(\vec{k}, \tau) \right\}, \quad \vec{k} = k \hat{k}. \quad (4)$$

Note that h is used to denote the trace of h_{ij} in both the real space and the Fourier space.

In spite of its wide-spread use, there are serious disadvantages associated with the synchronous gauge. Since the choice of the initial hypersurface and its coordinate assignments are arbitrary,

the synchronous gauge conditions do not fix the gauge degrees of freedom completely. Such residual gauge freedom is manifested in the spurious gauge modes contained in the solutions to the equations for the density perturbations. The appearance of these modes has caused some confusion over the years and prompted Bardeen (1980) to formulate alternative approaches that deal only with gauge-invariant quantities. Another difficulty with the synchronous gauge is that since the coordinates are defined by freely falling observers, coordinate singularities arise when two observers' trajectories intersect each other: a point in spacetime will have two coordinate labels. A different initial hypersurface of constant time has to be chosen to remove these singularities.

The conformal Newtonian gauge (also known as the longitudinal gauge) advocated by Mukhanov et al. (1992) is a particularly simple gauge to use for the scalar mode of metric perturbations. The perturbations are characterized by two scalar potentials ψ and ϕ which appear in the line element as

$$ds^2 = a^2(\tau) \left\{ -(1 + 2\psi)d\tau^2 + (1 - 2\phi)dx^i dx_i \right\}. \quad (5)$$

It should be emphasized that the conformal Newtonian gauge is a restricted gauge since the metric is applicable only for the scalar mode of the metric perturbations; the vector and the tensor degrees of freedom are eliminated from the beginning. Nonetheless, it can be easily generalized to include the vector and the tensor modes (Bertschinger 1995). The discussion here will be confined to the scalar perturbations only.

One advantage of working in this gauge is that the metric tensor $g_{\mu\nu}$ is diagonal. This simplifies the calculations and leads to simple geodesic equations (Ma & Bertschinger 1994a). Another advantage is that ψ plays the role of the gravitational potential in the Newtonian limit and thus has a simple physical interpretation. Moreover, the two scalar potentials ψ and ϕ in this gauge are related to the gauge-invariant variables Φ_A and Φ_H of Bardeen (1980) and Ψ and Φ of Kodama & Sasaki (1984) by the simple relation

$$\psi = \Phi_A = \Psi, \quad \phi = -\Phi_H = -\Phi. \quad (6)$$

No gauge modes are present in this gauge to obscure the meaning of the physical modes since the gauge freedom is completely fixed for $\Omega = 1$ aside from the addition of spatial constants to ψ and ϕ . The two potentials differ when the energy-momentum tensor $T^\mu{}_\nu$ contains a nonvanishing traceless and longitudinal component (see eq. [23d]).

3. Gauge Transformations

In this section we first derive the transformation law relating two arbitrary gauges. From it, the gauge transformation relating the synchronous gauge and the conformal Newtonian gauge is readily obtained.

A perturbed flat Friedmann-Robertson-Walker metric can be written in general as

$$\begin{aligned}
 g_{00} &= -a^2(\tau) \{1 + 2\psi(\vec{x}, \tau)\}, \\
 g_{0i} &= a^2(\tau) w_i(\vec{x}, \tau), \\
 g_{ij} &= a^2(\tau) \{[1 - 2\phi(\vec{x}, \tau)]\delta_{ij} + \chi_{ij}(\vec{x}, \tau)\}, \quad \chi_{ii} = 0
 \end{aligned} \tag{7}$$

where the functions ψ, ϕ, w_i and χ_{ij} represent metric perturbations about the Robertson-Walker spacetime and are assumed to be small compared with unity. The trace part of the perturbation to g_{ij} is absorbed in ϕ , and χ_{ij} is taken to be traceless.

Consider a general coordinate transformation from a coordinate system x^μ to another \hat{x}^μ

$$x^\mu \rightarrow \hat{x}^\mu = x^\mu + d^\mu(x^\nu). \tag{8}$$

We write the time and the spatial parts separately as

$$\begin{aligned}
 \hat{x}^0 &= x^0 + \alpha(\vec{x}, \tau), \\
 \hat{\vec{x}} &= \vec{x} + \vec{\nabla}\beta(\vec{x}, \tau) + \vec{\epsilon}(\vec{x}, \tau), \quad \vec{\nabla} \cdot \vec{\epsilon} = 0,
 \end{aligned} \tag{9}$$

where the vector \vec{d} has been decomposed into a longitudinal component $\vec{\nabla}\beta$ ($\vec{\nabla} \times \vec{\nabla}\beta = 0$) and a transverse component $\vec{\epsilon}$ ($\vec{\nabla} \cdot \vec{\epsilon} = 0$). The requirement that ds^2 be invariant under this coordinate transformation leads to

$$\hat{g}_{\mu\nu}(x) = g_{\mu\nu}(x) - g_{\mu\beta}(x)\partial_\nu d^\beta - g_{\alpha\nu}(x)\partial_\mu d^\alpha - d^\alpha\partial_\alpha g_{\mu\nu}(x) + O(d^2). \tag{10}$$

We note that both sides of this equation are evaluated at the same coordinate values x in the two gauges, which do not correspond to the same physical point in general. Assuming d^μ to be of the same order as the metric perturbations ψ, w_i, ϕ and χ_{ij} , the metric perturbations in the two coordinate systems are related to first order in the perturbed quantities by

$$\hat{\psi}(\vec{x}, \tau) = \psi(\vec{x}, \tau) - \dot{\alpha}(\vec{x}, \tau) - \frac{\dot{a}}{a}\alpha(\vec{x}, \tau), \tag{11a}$$

$$\hat{w}_i(\vec{x}, \tau) = w_i(\vec{x}, \tau) + \partial_i\alpha(\vec{x}, \tau) - \partial_i\dot{\beta}(\vec{x}, \tau) - \dot{\epsilon}_i(\vec{x}, \tau), \tag{11b}$$

$$\hat{\phi}(\vec{x}, \tau) = \phi(\vec{x}, \tau) + \frac{1}{3}\nabla^2\beta(\vec{x}, \tau) + \frac{\dot{a}}{a}\alpha(\vec{x}, \tau), \tag{11c}$$

$$\hat{\chi}_{ij}(\vec{x}, \tau) = \chi_{ij}(\vec{x}, \tau) - 2\left\{\left(\partial_i\partial_j - \frac{1}{3}\delta_{ij}\nabla^2\right)\beta(\vec{x}, \tau) + \frac{1}{2}(\partial_i\epsilon_j + \partial_j\epsilon_i)\right\}. \tag{11d}$$

We can further decompose the transformations of w_i and χ_{ij} above into longitudinal and transverse parts:

$$\begin{aligned}
 \hat{w}_i^\parallel(\vec{x}, \tau) &= w_i^\parallel(\vec{x}, \tau) + \partial_i\alpha(\vec{x}, \tau) - \partial_i\dot{\beta}(\vec{x}, \tau), \\
 \hat{w}_i^\perp(\vec{x}, \tau) &= w_i^\perp(\vec{x}, \tau) - \dot{\epsilon}_i(\vec{x}, \tau),
 \end{aligned} \tag{12}$$

and

$$\begin{aligned}
\hat{\chi}_{ij}^{\parallel}(\vec{x}, \tau) &= \chi_{ij}^{\parallel}(\vec{x}, \tau) - 2 \left(\partial_i \partial_j - \frac{1}{3} \delta_{ij} \nabla^2 \right) \beta(\vec{x}, \tau), \\
\hat{\chi}_{ij}^{\perp}(\vec{x}, \tau) &= \chi_{ij}^{\perp}(\vec{x}, \tau) - (\partial_i \epsilon_j + \partial_j \epsilon_i), \\
\hat{\chi}_{ij}^T(\vec{x}, \tau) &= \chi_{ij}^T(\vec{x}, \tau),
\end{aligned} \tag{13}$$

where $w_i = w_i^{\parallel} + w_i^{\perp}$, $\chi_{ij} = \chi_{ij}^{\parallel} + \chi_{ij}^{\perp} + \chi_{ij}^T$, and χ_{ij}^{\parallel} , χ_{ij}^{\perp} and χ_{ij}^T obey equation (2). Equations (11)–(13) describe the transformation of metric perturbations under a general infinitesimal coordinate transformation.

We can now use equations (11) to relate the scalar metric perturbations (ϕ, ψ) in the conformal Newtonian gauge to $h_{ij} = h \delta_{ij}/3 + h_{ij}^{\parallel}$ in the synchronous gauge. Let \hat{x}^{μ} denote the synchronous coordinates and x^{μ} the conformal Newtonian coordinates with $\hat{x}^{\mu} = x^{\mu} + d^{\mu}$. From equations (12) and (13), we find

$$\alpha(\vec{x}, \tau) = \dot{\beta}(\vec{x}, \tau) + \xi(\tau), \tag{14a}$$

$$\epsilon_i(\vec{x}, \tau) = \epsilon_i(\vec{x}), \tag{14b}$$

$$h_{ij}^{\parallel}(\vec{x}, \tau) = -2 \left(\partial_i \partial_j - \frac{1}{3} \delta_{ij} \nabla^2 \right) \beta(\vec{x}, \tau), \tag{14c}$$

$$\partial_i \epsilon_j + \partial_j \epsilon_i = 0, \tag{14d}$$

where $\xi(\tau)$ is an arbitrary function of time, reflecting the gauge freedom associated with the coordinate transformation: $\hat{x}^0 = x^0 + \xi(\tau)$, $\hat{x}^i = x^i$. This transformation corresponds to a global redefinition of the units of time with no physical significance; therefore we shall set $\xi = 0$ from now on. From equations (11a) and (11c) we then obtain

$$\begin{aligned}
\psi(\vec{x}, \tau) &= +\ddot{\beta}(\vec{x}, \tau) + \frac{\dot{a}}{a} \dot{\beta}(\vec{x}, \tau), \\
\phi(\vec{x}, \tau) &= -\frac{1}{6} h(\vec{x}, \tau) - \frac{1}{3} \nabla^2 \beta(\vec{x}, \tau) - \frac{\dot{a}}{a} \dot{\beta}(\vec{x}, \tau),
\end{aligned} \tag{15}$$

and β is determined by h^{\parallel} in equation (14c).

In terms of h and η introduced in equation (4), h_{ij}^{\parallel} in the synchronous gauge is given by

$$h_{ij}^{\parallel}(\vec{x}, \tau) = \int d^3 k e^{i\vec{k} \cdot \vec{x}} (\hat{k}_i \hat{k}_j - \frac{1}{3} \delta_{ij}) \left\{ h(\vec{k}, \tau) + 6\eta(\vec{k}, \tau) \right\}, \quad \vec{k} = k \hat{k}. \tag{16}$$

Comparing h_{ij}^{\parallel} in equations (14c) and (16), we can read off β :

$$\beta(\vec{x}, \tau) = \int d^3 k e^{i\vec{k} \cdot \vec{x}} \frac{1}{2k^2} \left\{ h(\vec{k}, \tau) + 6\eta(\vec{k}, \tau) \right\}. \tag{17}$$

Then from equations (15), the conformal Newtonian potentials ϕ and ψ are related to the synchronous potentials h and η in k -space by

$$\begin{aligned}
\psi(\vec{k}, \tau) &= \frac{1}{2k^2} \left\{ \ddot{h}(\vec{k}, \tau) + 6\ddot{\eta}(\vec{k}, \tau) + \frac{\dot{a}}{a} \left[\dot{h}(\vec{k}, \tau) + 6\dot{\eta}(\vec{k}, \tau) \right] \right\}, \\
\phi(\vec{k}, \tau) &= \eta(\vec{k}, \tau) - \frac{1}{2k^2} \frac{\dot{a}}{a} \left[\dot{h}(\vec{k}, \tau) + 6\dot{\eta}(\vec{k}, \tau) \right].
\end{aligned} \tag{18}$$

The other components of the metric perturbations, w_i, χ_{ij}^\perp , and χ_{ij}^T , are zero in both gauges.

4. Einstein Equations and Energy-Momentum Conservation

For a homogeneous Friedmann-Robertson-Walker universe with energy density $\bar{\rho}(\tau)$ and pressure $\bar{P}(\tau)$, the Einstein equations give the following evolution equations for the expansion factor $a(\tau)$:

$$\left(\frac{\dot{a}}{a}\right)^2 = \frac{8\pi}{3}Ga^2\bar{\rho} - \kappa, \quad (19)$$

$$\frac{d}{d\tau}\left(\frac{\dot{a}}{a}\right) = -\frac{4\pi}{3}Ga^2(\bar{\rho} + 3\bar{P}), \quad (20)$$

where the dots denote derivatives with respect to τ , and κ is positive, zero, or negative for a closed, flat, or open universe, respectively. We consider only models with total $\Omega = 1$ in this paper, so we set $\kappa = 0$. A cosmological constant is allowed through its inclusion in $\bar{\rho}$ and \bar{P} : $\bar{\rho}_\Lambda = \Lambda/8\pi G = -\bar{P}_\Lambda$. This is the only place that Λ enters in the entire set of calculations. It follows from equation (19) with $\kappa = 0$ that the expansion factor scales as $a \propto \tau$ in the radiation-dominated era, $a \propto \tau^2$ in the matter-dominated era, and $a \propto (\tau_\infty - \tau)^{-1}$ in a cosmological constant-dominated era (in the latter case, τ_∞ is the radius of the de Sitter event horizon).

We find it most convenient to solve the linearized Einstein equations in the two gauges in the Fourier space k . In the synchronous gauge, the scalar perturbations are characterized by $h(\vec{k}, \tau)$ and $\eta(\vec{k}, \tau)$ in equation (4). In terms of h and η , the time-time, longitudinal time-space, trace space-space, and longitudinal traceless space-space parts of the Einstein equations give the following four equations to linear order in k -space:

Synchronous gauge —

$$k^2\eta - \frac{1}{2}\frac{\dot{a}}{a}\dot{h} = 4\pi Ga^2\delta T^0_0(\text{Syn}), \quad (21a)$$

$$k^2\dot{\eta} = 4\pi Ga^2(\bar{\rho} + \bar{P})\theta(\text{Syn}), \quad (21b)$$

$$\ddot{h} + 2\frac{\dot{a}}{a}\dot{h} - 2k^2\eta = -8\pi Ga^2\delta T^i_i(\text{Syn}), \quad (21c)$$

$$\ddot{h} + 6\dot{\eta} + 2\frac{\dot{a}}{a}(\dot{h} + 6\dot{\eta}) - 2k^2\eta = -24\pi Ga^2(\bar{\rho} + \bar{P})\sigma(\text{Syn}). \quad (21d)$$

The label ‘‘Syn’’ is used to distinguish the components of the energy-momentum tensor in the synchronous gauge from those in the conformal Newtonian gauge. The variables θ and σ are defined as

$$(\bar{\rho} + \bar{P})\theta \equiv ik^j\delta T^0_j, \quad (\bar{\rho} + \bar{P})\sigma \equiv -(\hat{k}_i\hat{k}_j - \frac{1}{3}\delta_{ij})\Sigma^i_j, \quad (22)$$

and $\Sigma^i_j \equiv T^i_j - \delta^i_j T^k_k/3$ denotes the traceless component of T^i_j . Kodama & Sasaki (1984) define the anisotropic stress perturbation Π , related to our σ by $\sigma = 2\Pi\bar{P}/3(\bar{\rho} + \bar{P})$. When the different

components of matter and radiation (i.e., CDM, HDM, baryons, photons, and massless neutrinos) are treated separately, $(\bar{\rho} + \bar{P})\theta = \sum_i(\bar{\rho}_i + \bar{P}_i)\theta_i$ and $(\bar{\rho} + \bar{P})\sigma = \sum_i(\bar{\rho}_i + \bar{P}_i)\sigma_i$, where the index i runs over the particle species.

In the conformal Newtonian gauge, the first-order perturbed Einstein equations give

Conformal Newtonian gauge —

$$k^2\phi + 3\frac{\dot{a}}{a}\left(\dot{\phi} + \frac{\dot{a}}{a}\psi\right) = 4\pi Ga^2\delta T^0_0(\text{Con}), \quad (23a)$$

$$k^2\left(\dot{\phi} + \frac{\dot{a}}{a}\psi\right) = 4\pi Ga^2(\bar{\rho} + \bar{P})\theta(\text{Con}), \quad (23b)$$

$$\ddot{\phi} + \frac{\dot{a}}{a}(\dot{\psi} + 2\dot{\phi}) + \left(2\frac{\ddot{a}}{a} - \frac{\dot{a}^2}{a^2}\right)\psi + \frac{k^2}{3}(\phi - \psi) = \frac{4\pi}{3}Ga^2\delta T^i_i(\text{Con}), \quad (23c)$$

$$k^2(\phi - \psi) = 12\pi Ga^2(\bar{\rho} + \bar{P})\sigma(\text{Con}), \quad (23d)$$

where ‘‘Con’’ labels the conformal Newtonian coordinates.

Now we derive the transformation relating δT^μ_ν in the two gauges. For a perfect fluid of energy density ρ and pressure P , the energy-momentum tensor has the form

$$T^\mu_\nu = Pg^\mu_\nu + (\rho + P)U^\mu U_\nu, \quad (24)$$

where $U^\mu = dx^\mu/\sqrt{-ds^2}$ is the four-velocity of the fluid. The pressure P and energy density ρ of a perfect fluid at a given point are defined to be the pressure and energy density measured by a comoving observer at rest with the fluid at the instant of measurements. For a fluid moving with a small coordinate velocity $v^i \equiv dx^i/d\tau$, v^i can be treated as a perturbation of the same order as $\delta\rho = \rho - \bar{\rho}$, $\delta P = P - \bar{P}$, and the metric perturbations. Then to linear order in the perturbations the energy-momentum tensor is given by

$$\begin{aligned} T^0_0 &= -(\bar{\rho} + \delta\rho), \\ T^0_i &= (\bar{\rho} + \bar{P})v_i = -T^i_0, \\ T^i_j &= (\bar{P} + \delta P)\delta^i_j + \Sigma^i_j, \quad \Sigma^i_i = 0, \end{aligned} \quad (25)$$

where we have allowed an anisotropic shear perturbation Σ^i_j in T^i_j . As we shall see, since the photons are tightly coupled to the baryons before recombination, the dominant contribution to this shear stress comes from the neutrinos. We note that for a fluid, θ defined in equation (22) is simply the divergence of the fluid velocity: $\theta = ik^j v_j$.

The energy-momentum tensor $T^\mu_\nu(\text{Syn})$ in the synchronous gauge is related to $T^\mu_\nu(\text{Con})$ in the conformal Newtonian gauge by the transformation

$$T^\mu_\nu(\text{Syn}) = \frac{\partial \hat{x}^\mu}{\partial x^\sigma} \frac{\partial x^\rho}{\partial \hat{x}^\nu} T^\sigma_\rho(\text{Con}), \quad (26)$$

where \hat{x}^μ and x^μ denote the synchronous and the conformal Newtonian coordinates, respectively. It follows that to linear order, $T^0_0(\text{Syn}) = T^0_0(\text{Con})$, $T^0_j(\text{Syn}) = T^0_j(\text{Con}) + ik_j\alpha(\bar{\rho} + \bar{P})$, and

$T_j^i(\text{Syn}) = T_j^i(\text{Con})$, where $\alpha = \hat{x}^0 - x^0 = (\dot{h} + 6\dot{\eta})/2k^2$ in k -space from equations (14a) and (17). Let $\delta \equiv \delta\rho/\bar{\rho} = -\delta T^0_0/\bar{\rho}$. Evaluating the perturbations at the same spacetime coordinate values, we obtain

$$\delta(\text{Syn}) = \delta(\text{Con}) - \alpha \frac{\dot{\bar{\rho}}}{\bar{\rho}}, \quad (27a)$$

$$\theta(\text{Syn}) = \theta(\text{Con}) - \alpha k^2, \quad (27b)$$

$$\delta P(\text{Syn}) = \delta P(\text{Con}) - \alpha \dot{\bar{P}}, \quad (27c)$$

$$\sigma(\text{Syn}) = \sigma(\text{Con}). \quad (27d)$$

This transformation also applies to individual species when more than one particle species contributes to the energy-momentum tensor, provided that the appropriate $\bar{\rho}$ and \bar{P} are used for each component.

The non-relativistic fluid description is appropriate for the CDM and the baryon components. The photon and the neutrino components, however, can be appropriately described only by their full distribution functions in phase space. The energy-momentum tensor in this case is expressed through integrals over momenta of the distribution functions. We will discuss it in detail in §5.

The conservation of energy-momentum is a consequence of the Einstein equations. Let $w \equiv P/\rho$ describe the equation of state. Then the perturbed part of energy-momentum conservation equations

$$T^{\mu\nu}{}_{;\mu} = \partial_\mu T^{\mu\nu} + \Gamma^\nu_{\alpha\beta} T^{\alpha\beta} + \Gamma^\alpha_{\alpha\beta} T^{\nu\beta} = 0 \quad (28)$$

in k -space implies

Synchronous gauge —

$$\begin{aligned} \dot{\delta} &= -(1+w) \left(\theta + \frac{\dot{h}}{2} \right) - 3 \frac{\dot{a}}{a} \left(\frac{\delta P}{\delta \rho} - w \right) \delta, \\ \dot{\theta} &= -\frac{\dot{a}}{a} (1-3w)\theta - \frac{\dot{w}}{1+w} \theta + \frac{\delta P/\delta \rho}{1+w} k^2 \delta - k^2 \sigma, \end{aligned} \quad (29)$$

Conformal Newtonian gauge —

$$\begin{aligned} \dot{\delta} &= -(1+w) (\theta - 3\dot{\phi}) - 3 \frac{\dot{a}}{a} \left(\frac{\delta P}{\delta \rho} - w \right) \delta, \\ \dot{\theta} &= -\frac{\dot{a}}{a} (1-3w)\theta - \frac{\dot{w}}{1+w} \theta + \frac{\delta P/\delta \rho}{1+w} k^2 \delta - k^2 \sigma + k^2 \psi. \end{aligned} \quad (30)$$

These equations are valid for a single uncoupled fluid, or for the net (mass-averaged) δ and θ for all fluids. They need to be modified for individual components if the components interact with each other. An example is the baryonic fluid in our model, which couples to the photons before recombination via Thomson scattering. In the next section we will show that an extra term

representing momentum transfer between the two components needs to be added to the $\dot{\delta}$ equation for the baryons.

For the isentropic primordial perturbations considered in this paper, the equations above simplify since $\delta P = c_s^2 \delta \rho$, where $c_s^2 = dP/d\rho = w + \rho dw/d\rho$ is the adiabatic sound speed squared. For the photons and baryons (the only collisional fluid components with pressure), w is a constant ($w = 1/3$ for photons and $w \approx 0$ for baryons since they are nonrelativistic at the times of interest). Thus, $\delta P/\delta \rho - w = 0$. The entropy generated from the coupling of photons and baryons before recombination is accounted for by Thomson scattering terms added to their respective equations of motion in §§5.5–5.7. Even in the case of isocurvature baryon models, which may have large perturbations in the entropy per baryon ab initio, the corrections to $\delta P/\delta \rho = w$ are generally very small because of the large photon to baryon ratio.

5. Evolution Equations for Matter and Radiation

5.1. Phase Space and the Boltzmann Equation

A phase space is described by six variables: three positions x^i and their conjugate momenta P_i . Our treatment of phase space is based on the time-slicing of a definite gauge (synchronous or conformal Newtonian). Although this approach is not manifestly covariant, it yields correct results provided the gauge-dependent quantities are converted to observables at the end of the computation.

The conjugate momentum has the property that it is simply the spatial part of the 4-momentum with lower indices, i.e., for a particle of mass m , $P_i = mU_i$, where $U_i = dx_i/\sqrt{-ds^2}$. One can verify that the conjugate momentum is related to the proper momentum $p^i = p_i$ measured by an observer at a fixed spatial coordinate value by

$$\begin{aligned} P_i &= a(\delta_{ij} + \frac{1}{2}h_{ij})p^j, & \text{in synchronous gauge,} \\ P_i &= a(1 - \phi)p_i, & \text{in conformal Newtonian gauge.} \end{aligned} \tag{31}$$

In the absence of metric perturbations, Hamilton's equations imply that the conjugate momenta are constant, so the proper momenta redshift as a^{-1} .

The phase space distribution of the particles gives the number of particles in a differential volume $dx^1 dx^2 dx^3 dP_1 dP_2 dP_3$ in phase space:

$$f(x^i, P_j, \tau) dx^1 dx^2 dx^3 dP_1 dP_2 dP_3 = dN . \tag{32}$$

Importantly, f is a scalar and is invariant under canonical transformations. The zeroth-order phase space distribution is the Fermi-Dirac distribution for fermions (+ sign) and the Bose-Einstein

distribution for bosons (– sign):

$$f_0 = f_0(\epsilon) = \frac{g_s}{h_{\text{P}}^3} \frac{1}{e^{\epsilon/k_{\text{B}}T_0} \pm 1}, \quad (33)$$

where $\epsilon = a(p^2 + m^2)^{1/2} = (P^2 + a^2m^2)^{1/2}$, $T_0 = aT$ denotes the temperature of the particles today, the factor g_s is the number of spin degrees of freedom, and h_{P} and k_{B} are the Planck and the Boltzmann constants.

When the spacetime is perturbed, x^i and P_i remain canonically conjugate variables, with equations of motion given by Hamilton's equations (Bertschinger 1993). However, following common practice (e.g., Bond & Szalay 1983) we shall find it convenient to replace P_j by $q_j \equiv ap_j$ in order to eliminate the metric perturbations from the definition of the momenta. Moreover, we shall write the comoving 3-momentum q_j in terms of its magnitude and direction: $q_j = qn_j$ where $n^i n_i = \delta_{ij} n^i n^j = 1$. Thus, we change our phase space variables, replacing $f(x^i, P_j, \tau)$ by $f(x^i, q, n_j, \tau)$. While this is not a canonical transformation (i.e., q_i is not the momentum conjugate to x^i), it is perfectly valid provided that we correctly transform the momenta in Hamilton's equations. Note that we do not transform f . Because q_j are not the conjugate momenta, $d^3x d^3q$ is not the phase space volume element, and $f d^3x d^3q$ is not the particle number. In the conformal Newtonian gauge, for example, $(1 - 3\phi) f d^3x d^3q$ is the particle number; this result is sensible because $a(1 - \phi) dx^i$ is the proper distance.

In the perturbed case we shall continue to define ϵ as $a(\tau)$ times the proper energy measured by a comoving observer, $\epsilon = (q^2 + a^2m^2)^{1/2}$. This is related to the time component of the 4-momentum by $P_0 = -\epsilon$ in the synchronous gauge and $P_0 = -(1 + \psi)\epsilon$ in the conformal Newtonian gauge. For the CDM+HDM models we are interested in, the photons, the massless neutrinos, and the massive neutrinos at the time of neutrino decoupling are all ultra-relativistic particles, so ϵ in the unperturbed Fermi-Dirac and Bose-Einstein distributions can be simply replaced by the new variable q .

The general expression for the energy-momentum tensor written in terms of the distribution function and the 4-momentum components is given by

$$T_{\mu\nu} = \int dP_1 dP_2 dP_3 (-g)^{-1/2} \frac{P_\mu P_\nu}{P_0} f(x^i, P_j, \tau), \quad (34)$$

where g denotes the determinant of $g_{\mu\nu}$. It is convenient to write the phase space distribution as a zeroth-order distribution plus a perturbed piece in the new variables q and n_j :

$$f(x^i, P_j, \tau) = f_0(q) \left[1 + \Psi(x^i, q, n_j, \tau) \right]. \quad (35)$$

In the synchronous gauge, we have $(-g)^{-1/2} = a^{-4}(1 - \frac{1}{2}h)$ and $dP_1 dP_2 dP_3 = (1 + \frac{1}{2}h)q^2 dq d\Omega$ to linear order, where $h \equiv h_{ii}$ and $d\Omega$ is the solid angle associated with direction n_i . Using the relations $\int d\Omega n_i n_j = 4\pi\delta_{ij}/3$ and $\int d\Omega n_i = \int d\Omega n_i n_j n_k = 0$, it then follows from equation (34)

that

$$\begin{aligned}
T^0_0 &= -a^{-4} \int q^2 dq d\Omega \sqrt{q^2 + m^2 a^2} f_0(q) (1 + \Psi), \\
T^0_i &= a^{-4} \int q^2 dq d\Omega q n_i f_0(q) \Psi, \\
T^i_j &= a^{-4} \int q^2 dq d\Omega \frac{q^2 n_i n_j}{\sqrt{q^2 + m^2 a^2}} f_0(q) (1 + \Psi)
\end{aligned} \tag{36}$$

to linear order in the perturbations. Note that we have eliminated the explicit dependence on the metric perturbations in equation (34) by redefining P_i in terms of q and n_i . Note also that the comoving energy $\epsilon(q, \tau) = (q^2 + a^2 m^2)^{1/2}$ is used in the integrands but not in the argument of the unperturbed distribution function.

In the conformal Newtonian gauge, $(-g)^{-1/2} = a^{-4}(1 - \psi + 3\phi)$ and $dP_1 dP_2 dP_3 = (1 - 3\phi)q^2 dq d\Omega$. It then follows that the components of the energy-momentum tensor have the same form as in equations (36). Of course, it is understood that the variables q and n_i in this case are defined in relation to the conjugate momentum P_i in the conformal Newtonian coordinates, and not the synchronous coordinates. (They differ because comoving observers in the two coordinate systems are not the same.) The expansion factor a and Ψ are evaluated at the coordinates (x^i, τ) in the conformal Newtonian gauge.

The phase space distribution evolves according to the Boltzmann equation. In terms of our variables (x^i, q, n_j, τ) this is

$$\frac{Df}{d\tau} = \frac{\partial f}{\partial \tau} + \frac{dx^i}{d\tau} \frac{\partial f}{\partial x^i} + \frac{dq}{d\tau} \frac{\partial f}{\partial q} + \frac{dn_i}{d\tau} \frac{\partial f}{\partial n_i} = \left(\frac{\partial f}{\partial \tau} \right)_C, \tag{37}$$

where the right-hand side involves terms due to collisions, whose form depends on the type of particle interactions involved. From the geodesic equation

$$P^0 \frac{dP^\mu}{d\tau} + \Gamma^\mu_{\alpha\beta} P^\alpha P^\beta = 0, \tag{38}$$

it is straightforward to show that

$$\begin{aligned}
dq/d\tau &= -\frac{1}{2} q \dot{h}_{ij} n_i n_j && \text{in synchronous gauge,} \\
dq/d\tau &= q \dot{\phi} - \epsilon(q, \tau) n_i \partial_i \psi && \text{in conformal Newtonian gauge,}
\end{aligned} \tag{39}$$

and $dn_i/d\tau$ is $O(h)$. Since $\partial f/\partial n_i$ is also a first-order quantity, the term $(dn_i/d\tau)(\partial f/\partial n_i)$ in the Boltzmann equation can be neglected to first order. Then the Boltzmann equation in k -space can be written as

Synchronous gauge —

$$\frac{\partial \Psi}{\partial \tau} + i \frac{q}{\epsilon} (\vec{k} \cdot \hat{n}) \Psi + \frac{d \ln f_0}{d \ln q} \left[\dot{\eta} - \frac{\dot{h} + 6\dot{\eta}}{2} (\hat{k} \cdot \hat{n})^2 \right] = \frac{1}{f_0} \left(\frac{\partial f}{\partial \tau} \right)_C, \tag{40}$$

Conformal Newtonian gauge —

$$\frac{\partial \Psi}{\partial \tau} + i \frac{q}{\epsilon} (\vec{k} \cdot \hat{n}) \Psi + \frac{d \ln f_0}{d \ln q} \left[\dot{\phi} - i \frac{\epsilon}{q} (\vec{k} \cdot \hat{n}) \psi \right] = \frac{1}{f_0} \left(\frac{\partial f}{\partial \tau} \right)_C. \quad (41)$$

Equations (40) and (41) can also be derived using the canonical phase space variables x^i and P_j and Hamilton's equations (instead of the geodesic equation), followed by a transformation from P_j to qn_j .

The terms in the Boltzmann equation depend on the direction of the momentum \hat{n} only through its angle with \vec{k} . (We shall see that this is true of the collision term for photons as well as the convective and metric perturbation terms.) Therefore, if the momentum-dependence of the initial phase space perturbation is axially symmetric about \vec{k} , it will remain axially symmetric. If axially-asymmetric perturbations in the neutrinos or other collisionless particles are produced, they would generate no scalar metric perturbations and thus would have no effect on other species. Therefore, we shall assume that the initial momentum-dependence is axially symmetric so that Ψ depends on $\vec{q} = q\hat{n}$ only through q and $\hat{k} \cdot \hat{n}$. This assumption, which effectively reduces the dimensionality of phase space perturbations by one (after Fourier transforming on the spatial coordinates), has been made (implicitly, if not explicitly) in all previous studies of the evolution of scalar perturbations.

5.2. Cold Dark Matter

CDM interacts with other particles only through gravity and can be treated as a pressureless perfect fluid. The CDM particles can be used to define the synchronous coordinates and therefore have zero peculiar velocities in this gauge. Setting $\theta = \sigma = 0$ and $w = \dot{w} = 0$ in equations (29) leads to

Synchronous gauge —

$$\dot{\delta}_c = -\frac{1}{2} \dot{h}. \quad (42)$$

The CDM fluid velocity in the conformal Newtonian gauge, however, is not zero in general. In k -space, equations (30) give

Conformal Newtonian gauge —

$$\dot{\delta}_c = -\theta_c + 3\dot{\phi}, \quad \dot{\theta}_c = -\frac{\dot{a}}{a} \theta_c + k^2 \psi. \quad (43)$$

The subscript c in δ_c and θ_c denotes the cold dark matter.

5.3. Massless Neutrinos

The energy density and the pressure for massless neutrinos (labeled by subscripts ν) are $\rho_\nu = 3P_\nu = -T^0_0 = T^i_i$. From equations (36) the unperturbed energy density $\bar{\rho}_\nu$ and pressure \bar{P}_ν are given by

$$\bar{\rho}_\nu = 3\bar{P}_\nu = a^{-4} \int q^2 dq d\Omega q f_0(q), \quad (44)$$

and the perturbations of energy density $\delta\rho_\nu$, pressure δP_ν , energy flux δT^0_i , and shear stress $\Sigma^i_{\nu j} = T^i_{\nu j} - P_\nu \delta_{ij}$ are given by

$$\begin{aligned} \delta\rho_\nu &= 3\delta P_\nu = a^{-4} \int q^2 dq d\Omega q f_0(q) \Psi, \\ \delta T^0_i &= a^{-4} \int q^2 dq d\Omega q n_i f_0(q) \Psi, \\ \Sigma^i_{\nu j} &= a^{-4} \int q^2 dq d\Omega q (n_i n_j - \frac{1}{3} \delta_{ij}) f_0(q) \Psi. \end{aligned} \quad (45)$$

The unperturbed energy flux and shear stress are zero.

The Boltzmann equation simplifies for massless particles, for which $\epsilon = q$. To reduce the number of variables we integrate out the q -dependence in the neutrino distribution function and expand the angular dependence of the perturbation in a series of Legendre polynomials $P_l(\hat{k} \cdot \hat{n})$:

$$F_\nu(\vec{k}, \hat{n}, \tau) \equiv \frac{\int q^2 dq q f_0(q) \Psi}{\int q^2 dq q f_0(q)} \equiv \sum_{l=0}^{\infty} (-i)^l (2l+1) F_{\nu l}(\vec{k}, \tau) P_l(\hat{k} \cdot \hat{n}). \quad (46)$$

As noted in §5.1, the dependence on \hat{n} arises only through $\hat{k} \cdot \hat{n}$, so that a general distribution may be represented as in equation (46). The factor $(-i)^l (2l+1)$ is chosen to simplify the expansion of a plane wave: $F_\nu = \exp(-i\vec{k} \cdot \vec{x})$ with $\vec{x} = r(\tau)\hat{n}$ has expansion coefficients $F_{\nu l} = j_l(kr)$ given by spherical Bessel functions.

In terms of the new variable $F_\nu(\vec{k}, \hat{n}, \tau)$ and its harmonic expansion coefficients, the perturbations δ_ν , $\bar{\rho}_\nu$, θ_ν , and σ_ν (defined in eq. [22]) take the form

$$\begin{aligned} \delta_\nu &= \frac{1}{4\pi} \int d\Omega F_\nu(\vec{k}, \hat{n}, \tau) = F_{\nu 0}, \\ \theta_\nu &= \frac{3i}{16\pi} \int d\Omega (\vec{k} \cdot \hat{n}) F_\nu(\vec{k}, \hat{n}, \tau) = \frac{3}{4} k F_{\nu 1}, \\ \sigma_\nu &= -\frac{3}{16\pi} \int d\Omega \left[(\hat{k} \cdot \hat{n})^2 - \frac{1}{3} \right] F_\nu(\vec{k}, \hat{n}, \tau) = \frac{1}{2} F_{\nu 2}, \end{aligned} \quad (47)$$

where we have used $\rho_\nu = 3P_\nu$ for the massless neutrinos.

Integrating equations (40) and (41) over $q^2 dq q f_0(q)$ and dividing them by $\int q^2 dq q f_0(q)$, the Boltzmann equation for massless neutrinos becomes

$$\begin{aligned} \frac{\partial F_\nu}{\partial \tau} + ik\mu F_\nu &= -\frac{2}{3}\dot{h} - \frac{4}{3}(\dot{h} + 6\dot{\eta})P_2(\mu) \quad \text{in synchronous gauge,} \\ \frac{\partial F_\nu}{\partial \tau} + ik\mu F_\nu &= 4(\dot{\phi} - ik\mu\psi) \quad \text{in conformal Newtonian gauge,} \end{aligned} \quad (48)$$

where $\mu \equiv \hat{k} \cdot \hat{n}$ and $P_2(\mu) = \frac{1}{2}(3\mu^2 - 1)$ is the Legendre polynomial of degree 2. Substituting the Legendre expansion for F_ν and using the orthonormality of the Legendre polynomials and the recursion relation $(l+1)P_{l+1}(\mu) = (2l+1)\mu P_l(\mu) - lP_{l-1}(\mu)$, we obtain

Synchronous gauge —

$$\begin{aligned}\dot{\delta}_\nu &= -\frac{4}{3}\theta_\nu - \frac{2}{3}\dot{h}, \\ \dot{\theta}_\nu &= k^2 \left(\frac{1}{4}\delta_\nu - \sigma_\nu \right), \\ \dot{F}_{\nu 2} &= 2\dot{\sigma}_\nu = \frac{8}{15}\theta_\nu - \frac{3}{5}kF_{\nu 3} + \frac{4}{15}\dot{h} + \frac{8}{5}\dot{\eta}, \\ \dot{F}_{\nu l} &= \frac{k}{2l+1} \left[lF_{\nu(l-1)} - (l+1)F_{\nu(l+1)} \right], \quad l \geq 3.\end{aligned}\tag{49}$$

Conformal Newtonian gauge —

$$\begin{aligned}\dot{\delta}_\nu &= -\frac{4}{3}\theta_\nu + 4\dot{\phi}, \\ \dot{\theta}_\nu &= k^2 \left(\frac{1}{4}\delta_\nu - \sigma_\nu \right) + k^2\psi, \\ \dot{F}_{\nu l} &= \frac{k}{2l+1} \left[lF_{\nu(l-1)} - (l+1)F_{\nu(l+1)} \right], \quad l \geq 2.\end{aligned}\tag{50}$$

This set of equations governs the evolution of the phase space distribution of massless neutrinos. Note that a given mode F_l is coupled only to the $(l-1)$ and $(l+1)$ neighboring modes.

The Boltzmann equation (48) has been transformed into an infinite hierarchy of moment equations that must be truncated at some maximum multipole order l_{\max} . One simple but inaccurate method is to set $F_{\nu l} = 0$ for $l > l_{\max}$. The problem with this scheme is that the coupling of multipoles in equations (49) and (50) leads to the propagation of errors from l_{\max} to smaller l . Indeed, these errors can propagate to $l = 0$ in a time $\tau \approx l_{\max}/k$ and then reflect back to increasing l , leading to amplification of errors in the “square well” $0 \leq l \leq l_{\max}$.

An improved truncation scheme is based on extrapolating the behavior of $F_{\nu l}$ to $l = l_{\max} + 1$. For $l > 1$, the multipole moments are gauge-invariant and numerical solutions show that they exhibit damped oscillations reminiscent of spherical Bessel functions. In fact, if $\partial_\tau(\phi + \psi) = 0$ (choosing conformal Newtonian gauge for simplicity), the time dependence of the exact solution of the Boltzmann hierarchy is $F_{\nu l}(k, \tau) \propto j_l(k\tau)$ for $l > 0$. If we assume that this relation holds approximately for time-varying potentials, using a recurrence relation for spherical Bessel functions we get

$$F_{\nu(l_{\max}+1)} \approx \frac{(2l_{\max}+1)}{k\tau} F_{\nu l_{\max}} - F_{\nu(l_{\max}-1)}.\tag{51}$$

By numerically integrating the Boltzmann hierarchy with different choices of l_{\max} , we have found that this truncation scheme greatly improves on the simple truncation $F_{\nu(l_{\max}+1)} = 0$. However, time-variations of the potentials during the radiation-dominated era make even equation (51) a poor approximation if l_{\max} is chosen too small. We shall discuss in §8 our choices for l_{\max} .

5.4. Massive Neutrinos

Massive neutrinos also obey the collisionless Boltzmann equation. The evolution of the distribution function for massive neutrinos is, however, complicated by their nonzero mass. From equations (36), the unperturbed energy density and pressure for massive neutrinos (labeled by subscripts “ h ” for HDM) are given by

$$\bar{\rho}_h = a^{-4} \int q^2 dq d\Omega \epsilon f_0(q), \quad \bar{P}_h = \frac{1}{3} a^{-4} \int q^2 dq d\Omega \frac{q^2}{\epsilon} f_0(q), \quad (52)$$

where $\epsilon = \epsilon(q, \tau) = \sqrt{q^2 + m_\nu^2 a^2}$, while the perturbations are

$$\begin{aligned} \delta\rho_h &= a^{-4} \int q^2 dq d\Omega \epsilon f_0(q) \Psi, & \delta P_h &= \frac{1}{3} a^{-4} \int q^2 dq d\Omega \frac{q^2}{\epsilon} f_0(q) \Psi, \\ \delta T_{hi}^0 &= a^{-4} \int q^2 dq d\Omega q n_i f_0(q) \Psi, & \Sigma_{hj}^i &= a^{-4} \int q^2 dq d\Omega \frac{q^2}{\epsilon} (n_i n_j - \frac{1}{3} \delta_{ij}) f_0(q) \Psi. \end{aligned} \quad (53)$$

Since the comoving energy-momentum relation $\epsilon(q, \tau)$ depends on both the momentum and time, we can not simplify the calculations by integrating out the q -dependence in the distribution function as we did for the massless neutrinos above (see eq. [46]). Instead of applying equation (46), we expand the perturbation Ψ directly in a Legendre series

$$\Psi(\vec{k}, \hat{n}, q, \tau) = \sum_{l=0}^{\infty} (-i)^l (2l+1) \Psi_l(\vec{k}, q, \tau) P_l(\hat{k} \cdot \hat{n}). \quad (54)$$

Then the perturbed energy density, pressure, energy flux, and shear stress in k -space are given by

$$\begin{aligned} \delta\rho_h &= 4\pi a^{-4} \int q^2 dq \epsilon f_0(q) \Psi_0, \\ \delta P_h &= \frac{4\pi}{3} a^{-4} \int q^2 dq \frac{q^2}{\epsilon} f_0(q) \Psi_0, \\ (\bar{\rho}_h + \bar{P}_h) \theta_h &= 4\pi k a^{-4} \int q^2 dq q f_0(q) \Psi_1, \\ (\bar{\rho}_h + \bar{P}_h) \sigma_h &= \frac{8\pi}{3} a^{-4} \int q^2 dq \frac{q^2}{\epsilon} f_0(q) \Psi_2. \end{aligned} \quad (55)$$

Following the same procedure used for the massless neutrinos, the Boltzmann equation becomes

Synchronous gauge —

$$\begin{aligned} \dot{\Psi}_0 &= -\frac{qk}{\epsilon} \Psi_1 + \frac{1}{6} \dot{h} \frac{d \ln f_0}{d \ln q}, \\ \dot{\Psi}_1 &= \frac{qk}{3\epsilon} (\Psi_0 - 2\Psi_2), \\ \dot{\Psi}_2 &= \frac{qk}{5\epsilon} (2\Psi_1 - 3\Psi_3) - \left(\frac{1}{15} \dot{h} + \frac{2}{5} \dot{\eta} \right) \frac{d \ln f_0}{d \ln q}, \\ \dot{\Psi}_l &= \frac{qk}{(2l+1)\epsilon} [l\Psi_{l-1} - (l+1)\Psi_{l+1}], \quad l \geq 3. \end{aligned} \quad (56)$$

Conformal Newtonian gauge —

$$\begin{aligned}
 \dot{\Psi}_0 &= -\frac{qk}{\epsilon}\Psi_1 - \dot{\phi}\frac{d\ln f_0}{d\ln q}, \\
 \dot{\Psi}_1 &= \frac{qk}{3\epsilon}(\Psi_0 - 2\Psi_2) - \frac{\epsilon k}{3q}\psi\frac{d\ln f_0}{d\ln q}, \\
 \dot{\Psi}_l &= \frac{qk}{(2l+1)\epsilon}[l\Psi_{l-1} - (l+1)\Psi_{l+1}], \quad l \geq 2.
 \end{aligned}
 \tag{57}$$

Because of the q -dependence in these equations, it requires much more computing time to carry out the time integration for the massive neutrino. Bond & Szalay (1983) used a 16-point Gauss-Legendre method to approximate the q -integration. We do not use this method and instead perform the integration using sixth- or eighth-order Newton-Cotes quadrature (plus a remainder obtained by asymptotic expansion) with a q -grid of 128 q -points for every wavenumber k . We verified that this was enough to ensure a relative accuracy no worse than 10^{-4} by trying the integration with twice as many points. Then the perturbations $\delta\rho_h$, δP_h , θ_h , and σ_h that enter the right-hand side of the Einstein equations are calculated from equations (55) by numerically integrating Ψ_0 , Ψ_1 and Ψ_2 over q .

As with massless neutrinos, we must truncate the Boltzmann hierarchy for massive neutrinos. We have found the following scheme to work well:

$$\Psi_{\nu(l_{\max}+1)} \approx \frac{(2l_{\max}+1)\epsilon}{qk\tau} \Psi_{\nu l_{\max}} - \Psi_{\nu(l_{\max}-1)}.
 \tag{58}$$

Because the higher multipole moments decay rapidly once the neutrinos become nonrelativistic, it is possible to choose a much smaller l_{\max} for massive neutrinos than for massless ones.

5.5. Photons

Photons evolve differently before and after recombination. Before recombination, photons and baryons are tightly coupled, interacting mainly via Thomson scattering (and the electrostatic coupling of electrons and ions). In Thomson scatterings, the photon energy $h\nu$ is assumed to be much less than the electron rest mass $m_e \sim 0.511$ MeV and the recoil of the electron in the initial electron rest frame is neglected. (We are concerned with the period after neutrino decoupling, when $T < m_e$.) The classical differential cross section for Thomson scattering is given by $d\sigma/d\Omega = 3\sigma_T(1 + \cos^2\theta)/16\pi$, where $\sigma_T = 0.6652 \times 10^{-24}$ cm² and θ is the scattering angle (e.g., Jackson 1975). After recombination, the universe gradually becomes transparent to radiation and photons travel almost freely, although Thomson scattering continues to transfer energy and momentum between the photons and the matter.

The evolution of the photon distribution function can be treated in a similar way as the massless neutrinos, with the exception that the collisional terms on the right-hand side of the Boltzmann equation are now present and they depend on polarization. Photons propagating in direction \hat{n} are linearly polarized in the plane perpendicular to \hat{n} due to scattering of electron density perturbations with wavevector \vec{k} . We shall track both the sum (total intensity) and difference (Stokes parameter Q) of the phase space densities in the two polarization states for each \vec{k} and \hat{n} . We shall denote the former (the momentum-averaged total phase space density perturbation, summed over polarizations) by $F_\gamma(\vec{k}, \hat{n}, \tau)$, defined as in equation (46). Similarly, $G_\gamma(\vec{k}, \hat{n}, \tau)$ is the difference of the two linear polarization components. The linearized collision operators for Thomson scattering are (Bond & Efstathiou 1984, 1987; Kosowsky 1995)

$$\left(\frac{\partial F_\gamma}{\partial \tau}\right)_C = an_e \sigma_T \left[-F_\gamma + F_{\gamma 0} + 4\hat{n} \cdot \vec{v}_e - \frac{1}{2}(F_{\gamma 2} + G_{\gamma 0} + G_{\gamma 2}) P_2 \right], \quad (59)$$

$$\left(\frac{\partial G_\gamma}{\partial \tau}\right)_C = an_e \sigma_T \left[-G_\gamma + \frac{1}{2}(F_{\gamma 2} + G_{\gamma 0} + G_{\gamma 2})(1 - P_2) \right], \quad (60)$$

where n_e and \vec{v}_e are the proper mean density and velocity of the electrons. The terms proportional to P_2 come from the polarization-dependence of the Thomson cross section which, when averaged over incident directions, give an angular dependence $1 + \cos^2 \theta$ in the Thomson cross section even for unpolarized radiation. The anisotropic scattering and net polarization were both neglected by Peebles & Yu (1970); the former (but not the latter) were included by Wilson & Silk (1980, 1981) and most later workers.

Expanding $F_\gamma(\vec{k}, \hat{n}, \tau)$ and $G_\gamma(\vec{k}, \hat{n}, \tau)$ in Legendre series as in equation (46) and using the relations $\hat{n} \cdot \vec{v}_e = -(i\theta_b/k)P_1(\hat{k} \cdot \hat{n})$, $F_{\gamma 1} = 4\theta_\gamma/(3k)$, and $F_{\gamma 2} = 2\sigma_\gamma$, the collision operators can be rewritten as

$$\left(\frac{\partial F_\gamma}{\partial \tau}\right)_C = an_e \sigma_T \left[\frac{4i}{k}(\theta_\gamma - \theta_b)P_1 + \left(9\sigma_\gamma - \frac{1}{2}G_{\gamma 0} - \frac{1}{2}G_{\gamma 2}\right)P_2 - \sum_{l \geq 3}^{\infty} (-i)^l (2l+1)F_{\gamma l} P_l \right], \quad (61)$$

$$\left(\frac{\partial G_\gamma}{\partial \tau}\right)_C = an_e \sigma_T \left[\frac{1}{2}(F_{\gamma 2} + G_{\gamma 0} + G_{\gamma 2})(1 - P_2) - \sum_{l \geq 0}^{\infty} (-i)^l (2l+1)G_{\gamma l} P_l \right]. \quad (62)$$

The left-hand-side of the Boltzmann equation for F_γ and G_γ remain the same as for the massless neutrinos, so we obtain

Synchronous gauge —

$$\begin{aligned} \dot{\delta}_\gamma &= -\frac{4}{3}\theta_\gamma - \frac{2}{3}\dot{h}, \\ \dot{\theta}_\gamma &= k^2 \left(\frac{1}{4}\delta_\gamma - \sigma_\gamma \right) + an_e \sigma_T (\theta_b - \theta_\gamma), \\ \dot{F}_{\gamma 2} &= 2\dot{\sigma}_\gamma = \frac{8}{15}\theta_\gamma - \frac{3}{5}kF_{\gamma 3} + \frac{4}{15}\dot{h} + \frac{8}{5}\dot{\eta} - \frac{9}{5}an_e \sigma_T \sigma_\gamma + \frac{1}{10}an_e \sigma_T (G_{\gamma 0} + G_{\gamma 2}), \end{aligned}$$

$$\begin{aligned}
\dot{F}_{\gamma l} &= \frac{k}{2l+1} \left[lF_{\gamma(l-1)} - (l+1)F_{\gamma(l+1)} \right] - an_e\sigma_T F_{\gamma l}, \quad l \geq 3, \\
\dot{G}_{\gamma l} &= \frac{k}{2l+1} \left[lG_{\gamma(l-1)} - (l+1)G_{\gamma(l+1)} \right] + an_e\sigma_T \left[-G_{\gamma l} + \frac{1}{2} (F_{\gamma 2} + G_{\gamma 0} + G_{\gamma 2}) \left(\delta_{l0} + \frac{\delta_{l2}}{5} \right) \right],
\end{aligned} \tag{63}$$

Conformal Newtonian gauge —

$$\begin{aligned}
\dot{\delta}_\gamma &= -\frac{4}{3}\theta_\gamma + 4\dot{\phi}, \\
\dot{\theta}_\gamma &= k^2 \left(\frac{1}{4}\delta_\gamma - \sigma_\gamma \right) + k^2\psi + an_e\sigma_T(\theta_b - \theta_\gamma), \\
\dot{F}_{\gamma 2} &= 2\dot{\sigma}_\gamma = \frac{8}{15}\theta_\gamma - \frac{3}{5}kF_{\gamma 3} - \frac{9}{5}an_e\sigma_T\sigma_\gamma + \frac{1}{10}an_e\sigma_T(G_{\gamma 0} + G_{\gamma 2}), \\
\dot{F}_{\gamma l} &= \frac{k}{2l+1} \left[lF_{\gamma(l-1)} - (l+1)F_{\gamma(l+1)} \right] - an_e\sigma_T F_{\gamma l}, \quad l \geq 3 \\
\dot{G}_{\gamma l} &= \frac{k}{2l+1} \left[lG_{\gamma(l-1)} - (l+1)G_{\gamma(l+1)} \right] + an_e\sigma_T \left[-G_{\gamma l} + \frac{1}{2} (F_{\gamma 2} + G_{\gamma 0} + G_{\gamma 2}) \left(\delta_{l0} + \frac{\delta_{l2}}{5} \right) \right],
\end{aligned} \tag{64}$$

The subscripts γ and b refer to photons and baryons respectively.

We truncate the photon Boltzmann equations in a manner similar to massless neutrinos (eq. 51), except that Thomson opacity terms must be added. For $l = l_{\max}$ we replace equations (63) and (64) by

$$\begin{aligned}
\dot{F}_{\gamma l} &= kF_{\gamma(l-1)} - \frac{l+1}{\tau}F_{\gamma l} - an_e\sigma_T F_{\gamma l}, \\
\dot{G}_{\gamma l} &= kG_{\gamma(l-1)} - \frac{l+1}{\tau}G_{\gamma l} - an_e\sigma_T G_{\gamma l}.
\end{aligned} \tag{65}$$

5.6. Baryons

The baryons (and electrons) behave like a non-relativistic fluid described, in the absence of coupling to radiation, by the energy-momentum conservation equations (29) and (30) with $\delta P_b/\delta\rho_b = c_s^2 = w \ll 1$ and $\sigma = 0$. Since the baryons are very nonrelativistic after neutrino decoupling (the period of interest), we may neglect w and $\delta P/\delta\rho$ in all terms except the acoustic term $c_s^2 k^2 \delta$ (which is important for sufficiently high k ; note that the shear stress term $k^2\sigma$ is far smaller so we neglect it). Before recombination, however, the coupling of the baryons and the photons causes a transfer of momentum and energy between the two components.

From equation (22) the momentum density T^0_j for a given species is related to θ by $ik^j\delta T^0_j = (\bar{\rho} + \bar{P})\theta$. The momentum transfer into the photon component is represented by

$an_e\sigma_T(\theta_b - \theta_\gamma)$ of equations (63) and (64). Momentum conservation in Thomson scattering then implies that a term $(4\bar{\rho}_\gamma/3\bar{\rho}_b)an_e\sigma_T(\theta_\gamma - \theta_b)$ has to be added to the equation for $\dot{\theta}_b$ (where we have used $\bar{P}_b \ll \bar{\rho}_b$), so equations (29) and (30) are modified to become

Synchronous gauge —

$$\begin{aligned}\dot{\delta}_b &= -\theta_b - \frac{1}{2}\dot{h}, \\ \dot{\theta}_b &= -\frac{\dot{a}}{a}\theta_b + c_s^2 k^2 \delta_b + \frac{4\bar{\rho}_\gamma}{3\bar{\rho}_b}an_e\sigma_T(\theta_\gamma - \theta_b),\end{aligned}\tag{66}$$

Conformal Newtonian gauge —

$$\begin{aligned}\dot{\delta}_b &= -\theta_b + 3\dot{\phi}, \\ \dot{\theta}_b &= -\frac{\dot{a}}{a}\theta_b + c_s^2 k^2 \delta_b + \frac{4\bar{\rho}_\gamma}{3\bar{\rho}_b}an_e\sigma_T(\theta_\gamma - \theta_b) + k^2\psi.\end{aligned}\tag{67}$$

The square of the baryon sound speed is evaluated from

$$c_s^2 = \frac{\dot{P}_b}{\dot{\rho}_b} = \frac{k_B T_b}{\mu} \left(1 - \frac{1}{3} \frac{d \ln T_b}{d \ln a} \right),\tag{68}$$

where μ is the mean molecular weight (including free electrons and all ions of H and He) and, in the second equality, we have neglected the slow time variation of μ . (This approximation is adequate because even during recombination, when $\dot{\mu}$ is largest, the baryons contribute very little to the pressure of the photon-baryon fluid.) The baryon temperature evolves according to

$$\dot{T}_b = -2\frac{\dot{a}}{a}T_b + \frac{8}{3}\frac{\mu}{m_e}\frac{\bar{\rho}_\gamma}{\bar{\rho}_b}an_e\sigma_T(T_\gamma - T_b).\tag{69}$$

We assume that electron-ion collisions are rapid enough for kinetic equilibrium to hold with a common temperature T_b for electrons and all baryon species. Equation (69) follows from the first law of thermodynamics, $dQ = (3/2)d(P_b/\rho_b) + P_b d(1/\rho_b)$, with specific heating rate $\dot{Q} = 4(\bar{\rho}_\gamma/\bar{\rho}_b)an_e\sigma_T k_B(T_\gamma - T_b)$.

5.7. Tight-Coupling Approximation

Before recombination the Thomson opacity is so large that photons and baryons are tightly coupled, with $an_e\sigma_T \equiv \tau_c^{-1} \gg \dot{a}/a \sim \tau^{-1}$. The large values of the Thomson drag terms in equations (63)–(67) for $\dot{\theta}_\gamma$ and $\dot{\theta}_b$ make them numerically difficult to solve. Therefore, in this limit we shall follow the method of Peebles & Yu (1970) to obtain an alternative form of the equations

valid for $\tau_c/\tau \ll 1$ and $k\tau_c \ll 1$. The starting point is the exact equation obtained by combining the second of equations (64) and (67),

$$(1 + R)\dot{\theta}_b + \frac{\dot{a}}{a}\theta_b - c_s^2 k^2 \delta_b - k^2 R \left(\frac{1}{4} \delta_\gamma - \sigma_\gamma \right) + R(\dot{\theta}_\gamma - \dot{\theta}_b) = (1 + R)k^2 \psi, \quad (70)$$

where the right-hand side is included only in the conformal Newtonian gauge; in the synchronous gauge it is set to zero. We have defined $R \equiv (4/3)\bar{\rho}_\gamma/\bar{\rho}_b$. We shall see that the terms proportional to $(\dot{\theta}_\gamma - \dot{\theta}_b)$ and σ_γ may be neglected to lowest order in $\max[k\tau_c, \tau_c/\tau]$, with the result that the baryons and photons behave like a single coupled fluid with sound speed c_{pb} . (This should be distinguished from c_s , which denotes the sound speed for the baryons only and not that for the coupled photon-baryon fluid.) However, we require a more accurate approximation to account for the slip between the photon and baryon fluids.

From the second of equations (64), we have

$$\theta_b - \theta_\gamma = \tau_c \left[\dot{\theta}_\gamma - k^2 \left(\frac{1}{4} \delta_\gamma - \sigma_\gamma \right) - k^2 \psi \right] \quad (71)$$

in the conformal Newtonian gauge; in the synchronous gauge we simply set $\psi = 0$. Writing $\dot{\theta}_\gamma$ as $\dot{\theta}_b + (\dot{\theta}_\gamma - \dot{\theta}_b)$ and using equation (70), we get

$$\theta_b - \theta_\gamma = \frac{\tau_c}{1 + R} \left[-\frac{\dot{a}}{a}\theta_b + k^2 \left(c_s^2 \delta_b - \frac{1}{4} \delta_\gamma + \sigma_\gamma \right) + \dot{\theta}_\gamma - \dot{\theta}_b \right], \quad (72)$$

a result that is valid in both gauges. From the third of equations (63), we have

$$\sigma_\gamma = \frac{\tau_c}{9} \left(\frac{8}{3} \theta_\gamma + \frac{4}{3} \dot{h} + 8\dot{\eta} - 10\dot{\sigma}_\gamma - 3kF_{\gamma 3} \right) \quad (73)$$

in the synchronous gauge; in the conformal Newtonian gauge one sets $\dot{h} = \dot{\eta} = 0$. We see that $\sigma_\gamma \sim \delta_\gamma \times \max[k\tau_c, \tau_c/\tau]$ (the case $k\tau_c$ corresponding to acoustic oscillations with $\theta_\gamma \sim k\delta_\gamma$). Higher moments of the photon distribution are smaller by additional powers of $k\tau_c$ and we shall neglect them in the limit of tight coupling considered here. Our goal is to obtain equations for $\dot{\theta}_b$ and $\dot{\theta}_\gamma$ that are accurate to second order in τ_c .

To get an equation for $\dot{\theta}_b$ we differentiate equation (72) and use equation (70). Assuming that the gas is nearly fully ionized so that $n_e \propto a^{-3}$ and that the baryon temperature is approximately the radiation temperature implying $c_s^2 \propto a^{-1}$, we obtain

$$\dot{\theta}_b - \dot{\theta}_\gamma = \frac{2R}{1 + R} \frac{\dot{a}}{a} (\theta_b - \theta_\gamma) + \frac{\tau_c}{1 + R} \left[-\frac{\ddot{a}}{a} \theta_b - \frac{\dot{a}}{a} k^2 \left(\frac{1}{2} \delta_\gamma + \psi \right) + k^2 \left(c_s^2 \dot{\delta}_b - \frac{1}{4} \dot{\delta}_\gamma \right) \right] + O(\tau_c^2). \quad (74)$$

This equation holds in the conformal Newtonian gauge; in the synchronous gauge one should set $\psi = 0$. Note that $\dot{\delta}_b$ and $\dot{\delta}_\gamma$ are to be evaluated using the first of equations (63)–(67). Substituting equation (74) into equation (70) yields our desired equation of motion for $\max[k\tau_c, \tau_c/\tau] \ll 1$. If this condition is violated, then one should use the explicit form of equations (66) and (67) for $\dot{\theta}_b$.

To obtain an equation for $\dot{\theta}_\gamma$ we combine the explicit equations for $\dot{\theta}_\gamma$ and $\dot{\theta}_b$ to obtain the exact equation

$$\dot{\theta}_\gamma = -R^{-1} \left(\dot{\theta}_b + \frac{\dot{a}}{a} \theta_b - c_s^2 k^2 \delta_b \right) + k^2 \left(\frac{1}{4} \delta_\gamma - \sigma_\gamma \right) + \frac{(1+R)}{R} k^2 \psi \quad (75)$$

in conformal Newtonian gauge; in synchronous gauge one sets $\psi = 0$. For $\dot{\theta}_b$ we use the tight-coupling approximation (substituting eq. [74] into eq. [70]) at early times and the exact explicit equations (66) or (67) at late times. In practice, we switch to the explicit scheme for $\dot{\theta}_b$ when $T_b = 2 \times 10^4$ K; we switch to the explicit scheme for $\dot{F}_{\gamma l}$ for $l > 1$ and $T_b = 2 \times 10^5$ K (at earlier times these moments are set to zero). We have verified that these switches occur early enough to preserve good accuracy in the resulting photon phase space distribution.

5.8. Recombination

In order to compute the Thomson scattering terms in the equations of motion for photons and baryons we need to know the free electron density $n_e(\tau)$. Our treatment is based on Peebles (1968; see also Peebles 1993) with the addition of helium with mass fraction $Y = 0.23$. We summarize the procedure here.

At high temperatures, hydrogen and helium are both fully ionized. Because of its much larger ionization potentials, helium recombines while hydrogen is still fully ionized and the free electron density is substantial. Consequently, the helium recombination rates are much larger than the expansion rate until helium recombination is essentially complete, so that Saha ionization equilibrium is an excellent approximation. We define the helium ionization fractions $x_1 = n(\text{He}^+)/n(\text{He})$ and $x_2 = n(\text{He}^{++})/n(\text{He})$, where $n(\text{He})$ is the total number density of helium nuclei. The Saha equation is

$$\frac{n_e x_{n+1}}{x_n} = \frac{2g_{n+1}}{g_n} \left(\frac{m_e k_B T_b}{2\pi \hbar^2} \right)^{3/2} e^{-\chi_n/k_B T_b}, \quad (76)$$

where $n = 0$ or 1 ($x_0 \equiv 1 - x_1 - x_2$), the statistical weights for helium are $g_0 = g_1 = 1$ and $g_2 = 2$, and χ_n is the ionization potential from n -times ionized helium.

When hydrogen recombines, the rapidly declining free electron density leads to a breakdown of ionization equilibrium. One must integrate the appropriate kinetic equations. Because helium recombination is completed before hydrogen begins to recombine appreciably, it is sufficient now to treat the helium as being fully neutral. We define the ionization fraction of hydrogen as $x_H = n_e/n_H$ where n_H is the total number density of hydrogen nuclei. The ionization rate equation is (Peebles 1968; Spitzer 1978)

$$\frac{dx_H}{d\tau} = aC_r \left[\beta(T_b)(1 - x_H) - n_H \alpha^{(2)}(T_b) x_H^2 \right]. \quad (77)$$

The factor C_r is discussed below. The collisional ionization rate from the ground state is

$$\beta(T_b) = \left(\frac{m_e k_B T_b}{2\pi \hbar^2} \right)^{3/2} e^{-B_1/k_B T_b} \alpha^{(2)}(T_b), \quad (78)$$

where $B_1 = m_e e^4 / (2\hbar^2) = 13.6$ eV is the ground state binding energy, and the recombination rate to excited states is

$$\alpha^{(2)}(T_b) = \frac{64\pi}{(27\pi)^{1/2}} \frac{e^4}{m_e^2 c^3} \left(\frac{k_B T_b}{B_1} \right)^{-1/2} \phi_2(T_b), \quad \phi_2(T_b) \approx 0.448 \ln \left(\frac{B_1}{k_B T_b} \right). \quad (79)$$

This expression for $\phi_2(T_b)$ is a good approximation (better than one percent for $T_b < 6000$ K). At high temperatures this expression underestimates ϕ_2 but the neutral fraction is negligible so that we make no significant error by setting $\phi_2 = 0$ for $T_b > B_1/k_B = 1.58 \times 10^5$ K.

Recombination directly to the ground state is inhibited by the large Lyman alpha and Lyman continuum opacities. Net recombination must occur either by 2-photon decay from the $2s$ level, with a rate $\Lambda_{2s \rightarrow 1s} = 8.227 \text{ s}^{-1}$, or by the cosmological redshifting of Lyman alpha photons away from the line center. Peebles (1968) gives a detailed discussion of these atomic processes. The net recombination rate to the ground state is reduced by the fact that an atom in the $n = 2$ level may be ionized before it decays to the ground state. The reduction factor C_r is just the ratio of the net decay rate (including 2-photon decay and Lyman alpha production at the rate allowed by redshifting of photons out of the line) to the sum of the decay and ionization rates from the $n = 2$ level:

$$C_r = \frac{\Lambda_\alpha + \Lambda_{2s \rightarrow 1s}}{\Lambda_\alpha + \Lambda_{2s \rightarrow 1s} + \beta^{(2)}(T_b)}, \quad (80)$$

where

$$\beta^{(2)}(T_b) = \beta(T_b) e^{+h\nu_\alpha/k_B T_b}, \quad \Lambda_\alpha = \frac{8\pi \dot{a}}{a^2 \lambda_\alpha^3 n_{1s}}, \quad \lambda_\alpha = \frac{8\pi \hbar c}{3B_1} = 1.216 \times 10^{-5} \text{ cm}, \quad (81)$$

where $\nu_\alpha = c/\lambda_\alpha$. For $T_b \ll 10^5$ K, it is a very good approximation to replace the number density n_{1s} of hydrogen atoms in the $1s$ state by $(1 - x_H)n_H$.

We integrate equation (77) using a stable and accurate semi-implicit method with a large number of timesteps through recombination. Since the results are independent of the perturbations, we pre-compute the ionization history of a model and later use cubic splines interpolation to obtain $n_e(\tau)$ (including electrons from both hydrogen and helium) accurately during integration of the perturbation equations. The baryon temperature and sound speed are also pre-computed for cubic splines interpolation.

6. Microwave Background Anisotropy

Perturbations in the photon phase space distribution correspond to fluctuations in the cosmic microwave background radiation. In this section we show how to compute the anisotropy and its power spectrum from the results of integration of the Boltzmann equation.

The photon brightness temperature perturbation $\Delta \equiv \Delta T/T$ is defined by

$$f(x^i, q, n_j, \tau) = f_0 \left(\frac{q}{1 + \Delta} \right), \quad (82)$$

where $f_0(q)$ is the Bose-Einstein distribution of equation (33) with $\epsilon = q$. In general the anisotropy is a function of all phase-space variables: $\Delta = \Delta(x^i, q, n_j, \tau)$. From equation (35) we obtain, to first order in Ψ ,

$$\Delta = - \left(\frac{d \ln f_0}{d \ln q} \right)^{-1} \Psi. \quad (83)$$

Because the q -dependence of both the gravitational source terms and the linearized collision operator for Thomson scattering in the Boltzmann equation for Ψ (eqs. [40] and [41]) are both proportional to $d \ln f_0 / d \ln q$, Δ is independent of q . In other words, the perturbed microwave background radiation has a Planck spectrum with the brightness temperature at a given position depending only on the photon direction. (Scattering by a nonlinearly perturbed medium can, however, change the spectrum. An example is the Sunyaev-Zel'dovich effect occurring when the electron gas is much hotter than the radiation.) In the absence of spectral distortions, Δ is related very simply to the momentum-averaged phase space density perturbation (i.e., the relative energy density perturbation): $\Delta = \frac{1}{4} F_\gamma$. Note that Efstathiou & Bond (1984, 1987) and Bond (1995) define Δ to be the photon density perturbation, 4 times our definition.

To compute the anisotropy at a given spacetime point (x^i, τ) we superpose plane-wave contributions:

$$\Delta(\vec{x}, \hat{n}, \tau) = \int d^3 k e^{i\vec{k} \cdot \vec{x}} \Delta(\vec{k}, \hat{n}, \tau) \equiv \int d^3 k e^{i\vec{k} \cdot \vec{x}} \sum_{l=0}^{\infty} (-i)^l (2l+1) \Delta_l(\vec{k}, \tau) P_l(\hat{k} \cdot \hat{n}), \quad (84)$$

where $\Delta_l = \frac{1}{4} F_{\gamma l}$. The anisotropy at the origin may be expanded in spherical harmonics in the usual manner:

$$\Delta(\hat{n}) = \sum_{l=0}^{\infty} \sum_{m=-l}^l a_{lm} Y_{lm}(\hat{n}), \quad a_{lm} = (-i)^l 4\pi \int d^3 k Y_{lm}^*(\hat{k}) \Delta_l(\vec{k}, \tau). \quad (85)$$

The angular power spectrum of the anisotropy is defined by the covariance matrix of these expansion coefficients:

$$\langle a_{lm} a_{l'm'}^* \rangle = C_l \delta_{ll'} \delta_{mm'}, \quad (86)$$

where the angle brackets denote a theoretical ensemble average. The angular power spectrum is related to the angular two-point correlation function by

$$C(\theta) \equiv \langle \Delta(\hat{n}_1) \Delta(\hat{n}_2) \rangle = \frac{1}{4\pi} \sum_{l=0}^{\infty} (2l+1) C_l P_l(\hat{n}_1 \cdot \hat{n}_2) \quad (87)$$

where $\cos\theta = \hat{n}_1 \cdot \hat{n}_2$. Note that for $l > 1$ the anisotropy coefficients Δ_l are gauge-invariant. Excluding the monopole and dipole anisotropy, one obtains the same result for the angular power spectrum and angular correlation function in both synchronous and conformal Newtonian gauges.

The anisotropy coefficients $\Delta_l(\vec{k}, \tau)$ are random variables with amplitudes and phases depending on the initial perturbations. We assume that the initial conditions can be specified in terms of the conformal Newtonian gauge potential ψ as described in §7. Because the evolution equations for $F_{\gamma l}(\vec{k}, \tau)$ (and therefore Δ_l) are independent of \hat{k} , we may write

$$\Delta_l(\vec{k}, \tau) = \psi_i(\vec{k}) \Delta_l(k, \tau) , \quad (88)$$

where $\psi_i(\vec{k})$ is the initial perturbation and $\Delta_l(k, \tau)$ is the solution of the Boltzmann equation with $\psi_i = 1$ (i.e., it is the photon transfer function). Using the two-point correlation function of ψ_i in Fourier space,

$$\langle \psi_i(\vec{k}_1) \psi_i(\vec{k}_2) \rangle = P_\psi(k) \delta_D(\vec{k}_1 + \vec{k}_2) , \quad (89)$$

where δ_D is the Dirac delta function, we obtain the desired result

$$C_l = 4\pi \int d^3k P_\psi(k) \Delta_l^2(k, \tau) . \quad (90)$$

As an illustration of this formalism, consider the anisotropy on large angular scales arising from the Sachs-Wolfe effect. For isentropic perturbations on scales larger than the acoustic horizon at recombination, the present ($\tau = \tau_0$) anisotropy is related to the perturbation in ψ at recombination by $\Delta(\hat{n}, \tau_0) \approx \frac{1}{3}\psi(\vec{x} = -\vec{n}\chi, \tau_{\text{rec}})$ with $\chi = \tau_0 - \tau_{\text{rec}} \approx \tau_0$ (Sachs & Wolfe 1967). In this case the radiation transfer function is simply $\Delta_l(k, \tau) = \frac{1}{3}j_l(k\chi)$. Now suppose that the primeval spectrum of curvature fluctuations is a power-law, $P_\psi(k) = A\chi^3(k\chi)^{n-4} \propto k^{n-4}$ (with $n = 1$ corresponding to equal power on all scales, or the scale-invariant Harrison-Zel'dovich spectrum). The resulting angular power spectrum is

$$C_l \approx \frac{2^n \pi^3}{9} A \frac{\Gamma(3-n) \Gamma\left(\frac{2l+n-1}{2}\right)}{\Gamma^2\left(\frac{4-n}{2}\right) \Gamma\left(\frac{2l+5-n}{2}\right)} . \quad (91)$$

For $n = 1$ this reduces to $C_l \approx (8\pi^2/9)A/[l(l+1)]$.

7. Super-Horizon-Sized Perturbations and Initial Conditions

The evolution equations derived in the previous sections can be solved numerically once the initial perturbations are specified. We start the integration at early times when a given k -mode is still outside the horizon, i.e., $k\tau \ll 1$ where $k\tau$ is dimensionless. (We follow common usage in referring to waves with $k\tau < 1$ as being “outside the horizon” even though τ is more appropriately

called the comoving Hubble distance.) The behavior of the density fluctuations on scales larger than the horizon is gauge-dependent. The fluctuations can appear as growing modes in one coordinate system and as constant modes in another. As we will show in this section, this is exactly what occurs in the synchronous and the conformal Newtonian gauges.

We first review the synchronous gauge behavior, which has already been discussed by Press & Vishniac (1980) and Wilson & Silk (1981), although these authors did not include neutrinos. We are concerned only with the radiation-dominated era since the numerical integration for all the k -modes of interest will start in this era. At this early time, the massive neutrinos are relativistic, and the CDM and the baryons make a negligible contribution to the total energy density of the universe: $\bar{\rho}_{\text{total}} = \bar{\rho}_\nu + \bar{\rho}_\gamma$. The expansion rate is $\dot{a}/a = \tau^{-1}$. We can analytically extract the time-dependence of the metric and density perturbations h , η , δ , and θ on super-horizon scales ($k\tau \ll 1$) from equations (21), (49) and (63). The large Thomson damping terms in equations (63) drive the $l \geq 2$ moments of the photon distribution function $F_{\gamma l}$ and the polarization function $G_{\gamma l}$ to zero. Similarly, $F_{\nu l}$ for $l \geq 3$ can be ignored because they are smaller than $F_{\nu 2}$ by successive powers of $k\tau$. Equations (21a), (21c), (49), and (63) then give

$$\begin{aligned} \tau^2 \ddot{h} + \tau \dot{h} + 6[(1 - R_\nu)\delta_\gamma + R_\nu\delta_\nu] &= 0, \\ \dot{\delta}_\gamma + \frac{4}{3}\theta_\gamma + \frac{2}{3}\dot{h} &= 0, \quad \dot{\theta}_\gamma - \frac{1}{4}k^2\delta_\gamma = 0, \\ \dot{\delta}_\nu + \frac{4}{3}\theta_\nu + \frac{2}{3}\dot{h} &= 0, \quad \dot{\theta}_\nu - \frac{1}{4}k^2(\delta_\nu - 4\sigma_\nu) = 0, \\ \dot{\sigma}_\nu - \frac{2}{15}(2\theta_\nu + \dot{h} + 6\dot{\eta}) &= 0, \end{aligned} \tag{92}$$

where we have defined $R_\nu \equiv \bar{\rho}_\nu/(\bar{\rho}_\gamma + \bar{\rho}_\nu)$. For N_ν flavors of neutrinos ($N_\nu = 3$ in the standard model), after electron-positron pair annihilation and before the massive neutrinos become nonrelativistic, $\bar{\rho}_\nu/\bar{\rho}_\gamma = (7N_\nu/8)(4/11)^{4/3}$ is a constant.

To lowest order in $k\tau$, the terms $\propto k^2$ in equations (92) can be dropped, and we have $\dot{\theta}_\nu = \dot{\theta}_\gamma = 0$. Then these equations can be combined into a single fourth-order equation for h :

$$\tau \frac{d^4 h}{d\tau^4} + 5 \frac{d^3 h}{d\tau^3} = 0, \tag{93}$$

whose four solutions are power laws: $h \propto \tau^n$ with $n = 0, 1, 2$, and -2 . From equations (92) we also obtain

$$\begin{aligned} h &= A + B(k\tau)^{-2} + C(k\tau)^2 + D(k\tau), \\ \delta \equiv (1 - R_\nu)\delta_\gamma + R_\nu\delta_\nu &= -\frac{2}{3}B(k\tau)^{-2} - \frac{2}{3}C(k\tau)^2 - \frac{1}{6}D(k\tau), \\ \theta \equiv (1 - R_\nu)\theta_\gamma + R_\nu\theta_\nu &= -\frac{3}{8}Dk, \end{aligned} \tag{94}$$

and A , B , C , and D are arbitrary dimensionless constants. The other metric perturbation η can be found from equation (21a):

$$\eta = 2C + \frac{3}{4}D(k\tau)^{-1}. \tag{95}$$

Press & Vishniac (1980) derived a general expression for the time dependence of the four eigenmodes. They showed that of these four modes, the first two (proportional to A and B) are gauge modes that can be eliminated by a suitable coordinate transformation. The latter two modes (proportional to C and D) correspond to physical modes of density perturbations on scales larger than the Hubble distance in the radiation-dominated era. Both physical modes appear as growing modes in the synchronous gauge, but the $C(k\tau)^2$ mode dominates at later times. In fact, the mode proportional to D in the radiation-dominated era decays in the matter-dominated era (Ratra 1988). We choose our initial conditions so that only the fastest-growing physical mode is present (this is appropriate for perturbations created in the early universe), in which case $\theta_\gamma = \theta_\nu = \dot{\eta} = 0$ to lowest order in $k\tau$. To get nonzero starting values we must use the full equations (92) to obtain higher order terms for these variables. To get the perturbations in the baryons we impose the condition of constant entropy per baryon. Using all of these inputs, we obtain the leading-order behavior of super-horizon-sized perturbations in the synchronous gauge:

Synchronous gauge —

$$\begin{aligned} \delta_\gamma &= -\frac{2}{3}C(k\tau)^2, & \delta_c = \delta_b &= \frac{3}{4}\delta_\nu = \frac{3}{4}\delta_\gamma, \\ \theta_c &= 0, & \theta_\gamma = \theta_b &= -\frac{1}{18}C(k^4\tau^3), & \theta_\nu &= \frac{23 + 4R_\nu}{15 + 4R_\nu}\theta_\gamma, \\ \sigma_\nu &= \frac{4C}{3(15 + 4R_\nu)}(k\tau)^2, \\ h &= C(k\tau)^2, & \eta &= 2C - \frac{5 + 4R_\nu}{6(15 + 4R_\nu)}C(k\tau)^2. \end{aligned} \tag{96}$$

The initial conditions for the moments $\Psi_l, l \geq 1$, of the massive neutrino distribution can be related to Ψ_0 and the variables above by equations (56). To obtain the initial Ψ_0 , we can write the perturbed distribution function using equation (82) as $f = f_0(q)(1 + \Psi_0) = 2h_P^{-3}\{\exp[q/k(T + \Delta T)] + 1\}^{-1}$, where $\Delta T/T = \delta_\nu/4$ by the isentropic condition. Then using equations (56), we find the first three moments to be

$$\begin{aligned} \Psi_0 &= -\frac{1}{4}\delta_\nu \frac{d \ln f_0}{d \ln q}, \\ \Psi_1 &= -\frac{\epsilon}{3qk}\theta_\nu \frac{d \ln f_0}{d \ln q}, \\ \Psi_2 &= -\frac{1}{2}\sigma_\nu \frac{d \ln f_0}{d \ln q}, \end{aligned} \tag{97}$$

where the terms proportional to $m_\nu^2 a^2/q^2$ in Ψ_2 are dropped. The higher moments Ψ_l ($l \geq 3$) are negligible for $k\tau \ll 1$.

The initial conditions for the isentropic perturbations in the conformal Newtonian gauge can be obtained either by solving equations (23), (50), and (64), or using the transformations given by equations (18) and (27) (which enables us to relate the amplitudes in the two gauges). We find for the growing mode

Conformal Newtonian gauge —

$$\begin{aligned}
 \delta_\gamma &= -\frac{40C}{15 + 4R_\nu} = -2\psi, & \delta_c = \delta_b = \frac{3}{4}\delta_\nu = \frac{3}{4}\delta_\gamma, \\
 \theta_\gamma &= \theta_\nu = \theta_c = \theta_b = \frac{10C}{15 + 4R_\nu}(k^2\tau) = \frac{1}{2}(k^2\tau)\psi, \\
 \sigma_\nu &= \frac{4C}{3(15 + 4R_\nu)}(k\tau)^2 = \frac{1}{15}(k\tau)^2\psi, \\
 \psi &= \frac{20C}{15 + 4R_\nu}, & \phi = \left(1 + \frac{2}{5}R_\nu\right)\psi.
 \end{aligned} \tag{98}$$

The massive neutrino moments Ψ_l in this gauge are related to δ_ν , θ_ν , and σ_ν by the same equations (eq. [97]) as in the synchronous gauge. As claimed earlier, $\psi = \phi$ to zeroth order in $k\tau$ when no neutrinos are present (i.e., $R_\nu = 0$). If we characterize the perturbations in the conformal Newtonian gauge by the potential ψ , all matter and metric variables have a very simple form outside the horizon. The neutrino energy fraction R_ν enters only in the second potential ϕ as a result of the shear stress produced by the free-streaming neutrinos. Bardeen (1980) was concerned that a large shear stress would lead to large metric perturbations in the conformal Newtonian gauge. We see that this does not happen for isentropic growing-mode perturbations in which the shear stress arises solely due to the free-streaming of relativistic collisionless particles.

We see that δ grows with time in the synchronous gauge but remains a constant in the conformal Newtonian gauge before horizon crossing. Another significant difference is the larger value of the velocity perturbations for small $k\tau$ in the conformal Newtonian gauge. Physically, this difference arises because velocity perturbations vanish to lowest order in the synchronous gauge because the synchronous gauge spatial coordinates are Lagrangian coordinates for freely-falling observers (§2). The next-order velocity perturbations differ for the neutrinos and photons because these two fluids have effectively different equations of state: the neutrinos are collisionless while the photons behave like a perfect fluid due to their strong coupling to the baryons. In the conformal Newtonian gauge, the lowest-order velocity perturbations do not vanish because the conformal Newtonian gauge spatial coordinates are Eulerian coordinates. If we were to include the next-order corrections to θ proportional to $k^4\tau^3$, differences between the different fluid components would appear in equations (98).

In the conformal Newtonian gauge, the mode proportional to D in the synchronous gauge yields $\phi \propto \psi \propto \delta \propto (k\tau)^{-3}$. Thus, this mode corresponds to a decaying mode in the conformal Newtonian gauge even though it yields $\delta \propto (k\tau)$ in the synchronous gauge. The two gauge modes (A and B in eq. [94]) do not exist in the conformal Newtonian gauge.

8. Integration Results in Two CDM+HDM Models

We apply the results derived in the previous sections to two spatially flat cosmological models consisting of a mixture of CDM and HDM: (1) the “old” model with a neutrino fraction of $\Omega_\nu = 0.3$ and a corresponding neutrino mass of $m_\nu = 93.13 (\Omega_\nu h^2) \text{ eV} = 7 \text{ eV}$ (e.g. Davis et al 1992; Klypin et al 1993; Jing et al 1994; Cen & Ostriker 1994), and (2) the $\Omega_\nu = 0.2$ model ($m_\nu = 4.7 \text{ eV}$), which gives a better match to high-redshift observations (Ma & Bertschinger 1994b; Klypin et al 1995). Both models assume $\Omega_{\text{baryon}} = 0.05$ and $H_0 = 50 \text{ km s}^{-1} \text{ Mpc}^{-1}$.

In Fourier space, all the \vec{k} modes in the linearized Einstein, Boltzmann, and fluid equations evolve independently; thus the equations can be solved for one value of \vec{k} at a time. Moreover, all modes with the same k (the magnitude of the comoving wavevector) obey the same evolution equations. For purposes of computing matter transfer functions, we integrated the equations of motion numerically over the range $0.01 \text{ Mpc}^{-1} \leq k \leq 10 \text{ Mpc}^{-1}$ using 31 points evenly spaced in $\log_{10} k$ with an interval of $\Delta \log_{10} k = 0.1$. For computing microwave background anisotropy we used linear spacing in k with 5000 points up to $k = 0.5 \text{ Mpc}^{-1}$. The time integration was performed using the standard fifth- and sixth-order Runge-Kutta integrator `dverk` (obtained from `netlib@ornl.gov`). It began at conformal time $\tau_0 = 3 \times 10^{-4} \text{ Mpc}$ ($z \sim 10^9$), which was chosen so that the largest k (i.e. the smallest wavelength) was well outside the horizon at the onset of the integration. The full integration was carried to $z = 0$. The microwave background anisotropy calculations were performed on a Cray C-90 at the Pittsburgh Supercomputing Center, using a vectorized code that runs at about 570 MFlops per processor.

The Einstein equations provide redundant equations for the evolution of the metric perturbations. In the synchronous gauge we chose to use $a\dot{h}$ and η as the primary metric perturbation variables in the integration, and used equation (21b) and a combination of (21a) and (21c) as the evolution equations. In the conformal Newtonian gauge we integrated ϕ using equation (23b) and obtained ψ algebraically using (23d). In both gauges we used the time-time Einstein equation (eqs. [21a] and [23a]) to check integration accuracy. In the conformal Newtonian gauge it is possible to avoid integration of the metric perturbations altogether by combining equations (23a) and (23b) into an algebraic equation for ϕ . However, we found that this gave numerical difficulties because the initial value of ϕ has to be set with exquisite precision when $k\tau \ll 1$. We also found it necessary to obtain the initial θ 's from ϕ and the δ s in the combined constraint equations of (23a) and (23b). Although the analytical expressions in equations (98) are good approximations for $k\tau \ll 1$, slight deviations from the energy-momentum constraints was found to cause numerical difficulties.

In the computations of the potential and the density fields (shown in Figs. 2 – 4), the photon and the massless neutrino phase space distributions were expanded in Legendre series (see eq. [46]) with up to 2000 l -values in order to guarantee sufficient angular resolution. In the calculations of the temperature fluctuations (Fig. 1), we used the criterion $l_{\text{max}} = 1.5k\tau_{\text{max}} + 10$, where $a(\tau_{\text{max}}) = 1$ ($\tau_{\text{max}} \approx 12000$). The massive neutrinos are computationally expensive due to the momentum-dependence in equations (56) and (57). For all computations we performed the massive neutrino calculations on a grid of 128 q -points including 50 l -values for every q . Using our

truncation schemes given by equations (51), (58), and (65), truncating the Boltzmann hierarchies at $l_{\max} = 50$ for massive neutrinos and 2000 for the massless particles was adequate at better than the 0.1% level. We checked that all of our numerical approximations are adequate by increasing the grids of k , q , and l values as well as decreasing the integration timestep. We estimate that our final results have a relative accuracy better than 10^{-3} .

Figure 1 shows the angular power spectrum C_l (defined in §6) of the photon anisotropy in the CDM and the CDM+HDM models. We have assumed a scale-invariant spectrum of the primeval potential ψ normalized to $P_\psi(k) = k^{-3}$. Integrations using conformal Newtonian and synchronous gauges agree to better than 0.1%. Our results for CDM agree well with those of other workers who included accurate numerical integrations with massless neutrinos, polarization, and helium recombination (P. Steinhardt 1994, private communication; Hu et al. 1995). To our knowledge, ours are the first results for the CDM+HDM models including all of this physics and more as described in the preceding sections.

Inclusion of massive neutrinos increases the anisotropy at large l (by about 10 percent at the second and third acoustic peaks; see Fig. 1) because the decreased perturbation growth leads to a $\dot{\phi}$ contribution to the photon energy density fluctuation growth in equation (64). At the same time, the smaller ϕ at early times with massive neutrinos leads to a slight reduction in C_l below the first acoustic peak. The differences between the $\Omega_\nu = 0.2$ and 0.3 models are small (middle panel of Fig. 1). Polarization decreases the anisotropy at high l by increasing the photon shear stress σ_γ , leading to increased radiative diffusion (bottom panel of Fig. 1).

Figure 2 shows the time evolution of the metric perturbations $\phi(k, \tau)$ and $\psi(k, \tau)$ in the conformal Newtonian gauge for all 31 values of k in the $\Omega_\nu = 0.2$ CDM+HDM model. (The metric perturbations in the synchronous gauge have no simple physical interpretation, so we shall not bother presenting them.) The overall normalization was chosen arbitrarily (corresponding to $C = -1/6$ in eqs. [96] and [98]). The difference between ψ and ϕ in the radiation-dominated era is due to the shear stress contributed by the relativistic neutrinos (eq. [98]) which make up a fraction $R_\nu = 0.4052$ of the total energy density. On scales much smaller than the horizon, ψ corresponds to the Newtonian gravitational potential and $\phi = \psi$ in the matter-dominated era. As is well known, the potential is constant for growing-mode density perturbations of CDM in an Einstein-de Sitter universe. In a mixed dark matter model, however, the CDM density perturbation growth can be suppressed by the lack of growth of HDM perturbations so that ψ decays slowly.

The behavior of the metric perturbations can be understood as follows. All of the 31 k -modes are outside the horizon at early times when $\tau < 0.01$ Mpc. The horizon eventually “catches up” and a given k -mode crosses inside the horizon when $k\tau$ is about π . The modes with larger k (i.e., shorter wavelengths) enter the horizon earlier. If a given k -mode enters the horizon during the radiation-dominated era, the tight coupling between photons and baryons due to Thomson scattering induces damped acoustic oscillations in the conformal Newtonian gauge metric perturbations, which are exhibited in Figure 2 by the modes with $k > 0.1$ Mpc $^{-1}$. (In

fact, it is not the speed-of-light horizon that sets the scale for the oscillation and damping of the potential. Rather, as we show below, it is the acoustic horizon. These horizons are similar during the radiation-dominated era because the sound speed of the photon-baryon fluid (c_{pb} is $c/\sqrt{3}$.) The modes with $k < 0.1 \text{ Mpc}^{-1}$ enter the horizon during the matter-dominated era and do not oscillate acoustically because the Jeans wavenumber $k_J = (4\pi G\bar{\rho}a^2/c_{pb}^2)^{1/2}$ has then become much larger than the wavenumbers under investigation.

We can understand the damped oscillations more quantitatively by studying the Einstein equations (23) in the conformal Newtonian gauge. Analytical solutions can be found for a perfect fluid with no shear stress, in which case $\phi = \psi$. Using $c_{pb}^2 = \delta P/\delta\rho \approx \bar{p}/\bar{\rho}$ and $\dot{a}/a = 2\tau^{-1}/(1+3c_{pb}^2)$ (from eqs. [19] and [20]), equations (23) can be combined to yield

$$\tau^2 \ddot{\phi} + \frac{6(1+c_{pb}^2)}{1+3c_{pb}^2} \tau \dot{\phi} + (kc_{pb}\tau)^2 \phi = 0, \quad (99)$$

whose solutions (approximating c_{pb} as a constant) are Bessel functions with a power-law pre-factor:

$$\phi_{\pm} = (kc_{pb}\tau)^{-\nu} J_{\pm\nu}(kc_{pb}\tau), \quad \nu \equiv \frac{5+3c_{pb}^2}{2(1+3c_{pb}^2)}. \quad (100)$$

The ϕ_- solution corresponds to the decaying mode discussed in §6, so we shall ignore it. In the radiation-dominated era, $c_{pb}^2 = \frac{1}{3}$ and $\nu = \frac{3}{2}$, so that

$$\phi_+ = (kc_{pb}\tau)^{-3/2} J_{3/2}(kc_{pb}\tau) \propto \begin{cases} \text{constant}, & kc_{pb}\tau \ll 1, \\ a^{-2} \cos(kc_{pb}\tau), & kc_{pb}\tau \gg 1. \end{cases} \quad (101)$$

We refer to the damping for $kc_{pb}\tau \gg 1$ as acoustic damping; it corresponds to constant-amplitude acoustic oscillations in the density contrast of the photon-baryon fluid. The damped oscillations are apparent in Figure 2 for $\tau < \tau_{\text{eq}}$. The analytic solution holds of course only in the absence of neutrinos; obtaining the correct amplitudes for ψ and ϕ in CDM+HDM models shown in Figure 2 required the full integration discussed in this paper.

After the universe becomes matter-dominated, acoustic damping of the potential ceases, and the only physical process causing the potential to change is the free-streaming damping of perturbations in the massive neutrinos. We shall discuss this further after examining the evolution of the density perturbations.

Figure 3 shows the evolution of the density perturbations for the five particle species in the $\Omega_\nu = 0.2$ CDM+HDM model in the two gauges from our numerical integration. Three wavenumbers are plotted: $k = 0.01 \text{ Mpc}^{-1}$ (Fig. 3a), $k = 0.1 \text{ Mpc}^{-1}$ (Fig. 3b), and $k = 1.0 \text{ Mpc}^{-1}$ (Fig. 3c). Each mode is normalized with the same initial amplitude for ϕ as in Figure 2. There are several notable features:

Before horizon crossing —

(1) The initial amplitudes of the δ 's are related by the isentropic initial conditions: $\delta_\gamma = \delta_\nu = \delta_h = 4\delta_b/3 = 4\delta_c/3$. The behavior of δ outside the horizon is strongly gauge-dependent.

In the synchronous gauge, Figure 3 shows that all the δ 's before horizon crossing in the radiation-dominated era grow as a^2 . This confirms equations (96) since $a(\tau) \propto \tau$ at this time. It is straightforward to show that in the matter-dominated era (for $\Omega=1$), $\delta \propto \tau^2 \propto a$ for all modes before horizon crossing. In the conformal Newtonian gauge, the δ 's remain constant outside the horizon as derived in equations (98).

After horizon crossing —

(2) The perturbations come into causal contact after horizon crossing and become nearly independent of the coordinate choices. As Figure 3 shows, δ_c , δ_b , and δ_h in the two gauges are almost identical at late times. For CDM, the k -modes that enter the horizon during the radiation-dominated era behave very differently from those entering in the matter-dominated era. The critical scale separating the two is the horizon distance at the epoch of radiation-matter equality ($a_{\text{eq}} \sim 2 \times 10^{-4} \Omega h^2$): $k_{\text{eq}} = 2\pi/\tau_{\text{eq}} \sim 0.1 \text{ Mpc}^{-1}$ for our parameters. For the modes with $k > 0.1$, horizon crossing occurs when the energy density of the universe is dominated by radiation; thus the fluctuations in the CDM can not grow appreciably during this time. For the photons and the baryons, the important scale is the horizon size at recombination ($a_{\text{rec}} \sim 10^{-3}$): $k_{\text{rec}} = 2\pi/\tau_{\text{rec}} \sim 0.025 \text{ Mpc}^{-1}$. The modes with $k > 0.025$ (see Figs. 3b and 3c) enter the horizon before recombination, so the photons (long-dashed curves) and baryons (dash-dotted curves) oscillate acoustically while they are coupled by Thomson scattering. The coupling is not perfect. The friction of the photons dragging against the baryons leads to Silk damping (Silk 1968), which is prominent in Figure 3c at $a \sim 10^{-3.5}$. The baryons decouple from the photons at recombination and then fall very quickly into the potential wells formed around the CDM, resulting in the rapid growth of δ_b in Figures 3b and 3c.

(3) Neutrinos decouple from other species at $T \sim 1 \text{ MeV}$ and $a \sim 10^{-10}$. At this early time, both the massless and the eV-range massive neutrinos behave like relativistic collisionless particles. The massive neutrinos become non-relativistic when $3k_{\text{B}}T_{\nu} \sim m_{\nu}$, corresponding to $a_{\text{nr}} \sim 10^{-4}$ for 4.7 eV neutrinos. Close inspection of the figures at $a \approx a_{\text{nr}}$ reveals that δ_h (short-dashed curve) is indeed making a gradual transition from the upper line for the radiation fields to the lower line for the matter fields. Although the Jeans length of a fluid is not well defined for collisionless particles such as the neutrinos, the criterion for free-streaming damping is similar to the Jeans criterion for gravitational stability: free-streaming is important for $k > k_{\text{fs}}$, where $k_{\text{fs}}^2(a) = 4\pi G \bar{\rho} a^2 / v_{\text{med}}^2$ and v_{med} is the median neutrino speed. When the neutrinos are relativistic, $v \sim 1$ and $k_{\text{fs}}(a) \propto a^{-1}$ for $a < a_{\text{eq}}$. After the neutrinos become non-relativistic, the median neutrino speed is $v_{\text{med}} = 3k_{\text{B}}T_{0,\nu}/a m_{\nu} = 15a^{-1}(m_{\nu}/10 \text{ eV})^{-1} \text{ km s}^{-1}$. In the matter-dominated era, we have $4\pi G \bar{\rho} a^2 = \frac{3}{2} H_0^2 a^{-1}$ from the Friedmann equation, and therefore

$$k_{\text{fs}}(a) = 8 a^{1/2} \left(\frac{m_{\nu}}{10 \text{ eV}} \right) h \text{ Mpc}^{-1}. \quad (102)$$

In Figure 3a, since horizon crossing occurs when the free-streaming effect is already unimportant, the evolution of δ_h is very similar to that of CDM. In Figures 3b and 3c, however, the free streaming effect is evident and the growth of δ_h is suppressed until $k_{\text{fs}}(a)$ grows to $\sim k$. After

$k_{\text{fs}}(a) > k$, δ_h can grow again and catch up to δ_c . Since $k_{\text{fs}} \propto a^{1/2}$, the larger k modes suffer more free-streaming damping and δ_h can not grow until later times. The damping in δ_h also affects the growth of δ_c , slowing it down more for larger Ω_ν compared to the pure CDM model. This effect is apparent in the $z = 0$ power spectra of the pure CDM and the two CDM+HDM models in Figure 4. Contrary to previous figures, the curves in Figure 4 are normalized to the COBE-compatible rms quadrupole moment of $Q_{\text{rms-PS}} = 17.6 \mu K$ (Bennett et al. 1994).

9. Summary

The purpose of this paper was to present in both the synchronous and the conformal Newtonian gauges a complete discussion of the linear theory of scalar gravitational perturbations that is applicable to any flat CDM, HDM or CDM+HDM model (including a possible cosmological constant). For historical reasons, most calculations of linear fluctuation growth have been carried out in the synchronous gauge. The conformal Newtonian gauge, however, offers an alternative that is free of the gauge ambiguities and coordinate singularities associated with the synchronous gauge. We derived the coordinate transformation relating the two gauges and presented in parallel in both gauges the complete set of evolution equations: the Einstein equations for the metric perturbations, the Boltzmann equations for the photon and neutrino phase space distributions, and the fluid equations for CDM and baryons. A detailed discussion of the microwave background anisotropy calculations was also presented. Care was taken to include all important higher moments of the neutrino phase space distribution and the effects of helium recombination and photon polarization.

We solved the linear theory in the standard CDM model and two spatially flat CDM+HDM models with $\Omega_\nu = 0.2$ and 0.3 , assuming a scale-invariant spectrum of isentropic primordial fluctuations. (The baryon fraction was taken to be $\Omega_{\text{baryon}} = 0.05$ and $H_0 = 50 \text{ km s}^{-1} \text{ Mpc}^{-1}$.) The evolution of the metric perturbations and the density fields for all five particle species were presented, along with the first accurate calculations of the photon anisotropy power spectrum in CDM+HDM models. We also illustrated the gauge dependence of the density fields before horizon crossing and discussed the physical interpretation of the results.

Interested users may obtain our programs to integrate the perturbation equations at <http://arcturus.mit.edu/cosmics>.

We thank Uros Seljak, Alan Guth, Douglas Scott, and Martin White for helpful comments. We particularly thank Marie Machacek for a careful reading of the manuscript, Paul Steinhardt for pointing out the importance of photon polarization, and Paul Bode for his assistance in preparing a portable numerical package. This work was supported by NSF grant AST-9318185, NASA grants NAGW-2807 and NAG5-2816, and DOE grant DE-AC02-76ER03069. Supercomputing

time was generously provided by the National Center for Supercomputing Applications and the Pittsburgh Supercomputing Center. C.-P. Ma acknowledges Fellowship support from the Division of Physics, Mathematics, and Astronomy at Caltech. E.B. would like to thank John Bahcall for his hospitality at the Institute for Advanced Study, where part of this work was performed.

REFERENCES

- Bardeen, J. M. 1980, *Phys. Rev.*, D22, 1882
- Bennett, C. L. et al. 1994, 436, 423
- Bertschinger, E. 1993, in *Statistical Description of Transport in Plasma, Astro-, and Nuclear Physics*, ed. J. Misguich, G. Pelletier, & P. Schuck, (Nova Science, Commack, NY), 193
- Bertschinger, E. 1995, to appear in *Proceedings of Les Houches School, Session LX*, ed. R. Schaeffer (Elsevier Science, Netherlands)
- Bond, J. R. 1995, to appear in *Proceedings of Les Houches School, Session LX*, ed. R. Schaeffer (Elsevier Science, Netherlands)
- Bond, J. R., & Efstathiou, G. 1984, *ApJ*, 285, L45
- Bond, J. R., & Efstathiou, G. 1987, *MNRAS*, 226, 655
- Bond, J. R., & Szalay, A. 1983, *ApJ*, 276, 443
- Cen, R., & Ostriker, J. P. 1994, *ApJ*, 431, 451
- Davis, M., Summers, F. J., & Schlegel, D. 1992, *Nature*, 359, 393
- Durrer, R. 1989, *A&A*, 208, 1
- Durrer, R. 1993, ZU-TH14/92, preprint
- Efstathiou, G. 1990, in *Physics of the Early Universe: Proceedings of the 36th Scottish Universities Summer School in Physics*, ed. J. A. Peacock, A. E. Heavens, & A. T. Davies (New York: Adam Hilger), 361
- Holtzman, J. A. 1989, *ApJS*, 71, 1
- Hu, W., Scott, D., Sugiyama, N., & White, M. 1995, preprint astro-ph/9505043
- Jackson, J. D. 1975, *Classical Electrodynamics* (Wiley, New York)
- Jing, Y. P., Mo, H. J., Börner, G., & Fang, L. Z. 1994, *å*, 284, 703
- Klypin, A., Holtzman, J. A., Primack, J. R., & Regos, E. 1993, *ApJ*, 416, 1
- Klypin, A., Borgani, S., Holtzman, J. A., & Primack, J. R. 1995, *ApJ*, 444, 1
- Kodama, H., & Sasaki, M. 1984, *Prog. Theo. Phys. Suppl.* 78, 1
- Kosowsky, A. 1995, preprint astro-ph/9501045
- Lifshitz, E. M. 1946, *J. Phys. USSR*, 10, 116
- Lifshitz, E. M., & Khalatnikov, I. M. 1963, *Adv. Phys.*, 12, 185
- Ma, C.-P. 1994, to appear in *Dark Matter*, ed. S. Holt (New York: American Institute of Physics), astro-ph/9412068
- Ma, C.-P., & Bertschinger, E. 1994a, *ApJ*, 429, 22

- Ma, C.-P., & Bertschinger, E. 1994b, *ApJ*, 434, L5
- Mukhanov, V. F., Feldman, H. A., & Brandenberger, R. 1992, *Phys. Rep.*, 215, 206
- Peebles, P. J. E. 1968, *ApJ*, 153, 1
- Peebles, P. J. E. 1980, *The Large-Scale Structure of the Universe* (Princeton University Press, Princeton)
- Peebles, P. J. E. 1993, *Principles of Physical Cosmology* (Princeton University Press, Princeton)
- Peebles, P. J. E., & Yu, J. T. 1970, *ApJ*, 162, 815
- Press, W. H., & Vishniac, E. T. 1980, *ApJ*, 239, 1
- Primack, J. R., Holtzman, J., Klypin, A., & Caldwell, D. O. 1995, *Phys. Rev. Lett.* 74, 2160
- Ratra, B. 1988, *Phys. Rev.*, D38, 2399
- Sachs, R. K., & Wolfe, A. M. 1967, *ApJ*, 147, 73
- Silk, J. 1968, *ApJ*, 151, 459
- Spitzer, L. 1978, *Physical Processes in the Interstellar Medium*, (Wiley, New York)
- Stompor, R. 1994, *A&A*, 287, 693
- Sugiyama, N., & Gouda, N. 1992, *Prog. Theo. Phys.*, 88, 803
- Vittorio, N., & Silk, J. 1984, *ApJ*, 285, L39
- Vittorio, N., & Silk, J. 1992, *ApJ*, 385, L9
- Weinberg, S. 1972, *Gravitation and Cosmology* (Wiley, New York)
- White, M., Scott, D., & Silk, J. 1994, *ARA&A*, 32, 319
- Wilson, M. L., & Silk, J. 1980, *Phys. Scripta*, 21, 708
- Wilson, M. L., & Silk, J. 1981, *ApJ*, 243, 14
- Xiang, S., & Kiang, T. 1992, *MNRAS*, 259, 761

10. Figure Captions

Fig. 1: Top: The angular power spectrum C_l of the photon anisotropy (including polarization) in the CDM (solid), the $\Omega_\nu = 0.2$ CDM+HDM (dashed), and the $\Omega_\nu = 0.3$ CDM+HDM (dotted) models. Middle: The ratio of C_l for the CDM+HDM models relative to the CDM (dashed for $\Omega_\nu = 0.2$; dotted for $\Omega_\nu = 0.3$). Bottom: The fractional difference in C_l with and without polarization for the three models.

Fig. 2: The scalar metric perturbations $\phi(k, \tau)$ and $\psi(k, \tau)$ in the conformal Newtonian gauge in the $\Omega_\nu = 0.2$ CDM+HDM model. The 31 curves from left to right correspond to 31 values of k between 10.0 Mpc^{-1} and 0.01 Mpc^{-1} . The labels τ_{nr} , τ_{eq} and τ_{rec} indicate, respectively, the time the 4.7 eV neutrinos become non-relativistic, the matter-radiation equality time, and the recombination time.

Fig. 3: Evolution of the density fields in the synchronous gauge (top panels) and the conformal Newtonian gauge (bottom panels) in the $\Omega_\nu = 0.2$ CDM+HDM model for 3 wavenumbers $k = 0.01$ (Fig. 3a), 0.1 (Fig. 3b) and 1.0 (Fig. 3c) Mpc^{-1} . In each figure, the five lines represent $\delta_c, \delta_b, \delta_\gamma, \delta_\nu$ and δ_h for the CDM (solid), baryon (dash-dotted), photon (long-dashed), massless neutrino (dotted), and massive neutrino (short-dashed) components, respectively.

Fig. 4: The $z = 0$ power spectra for the pure CDM (solid), the $\Omega_\nu = 0.2$ CDM+HDM (dashed), and the $\Omega_\nu = 0.3$ CDM+HDM (dotted) models. In the mixed models, the upper curve is for the CDM component and the lower one is for the HDM. The COBE-compatible quadrupole moment of $Q_{\text{rms-PS}} = 17.6 \mu K$ is used.

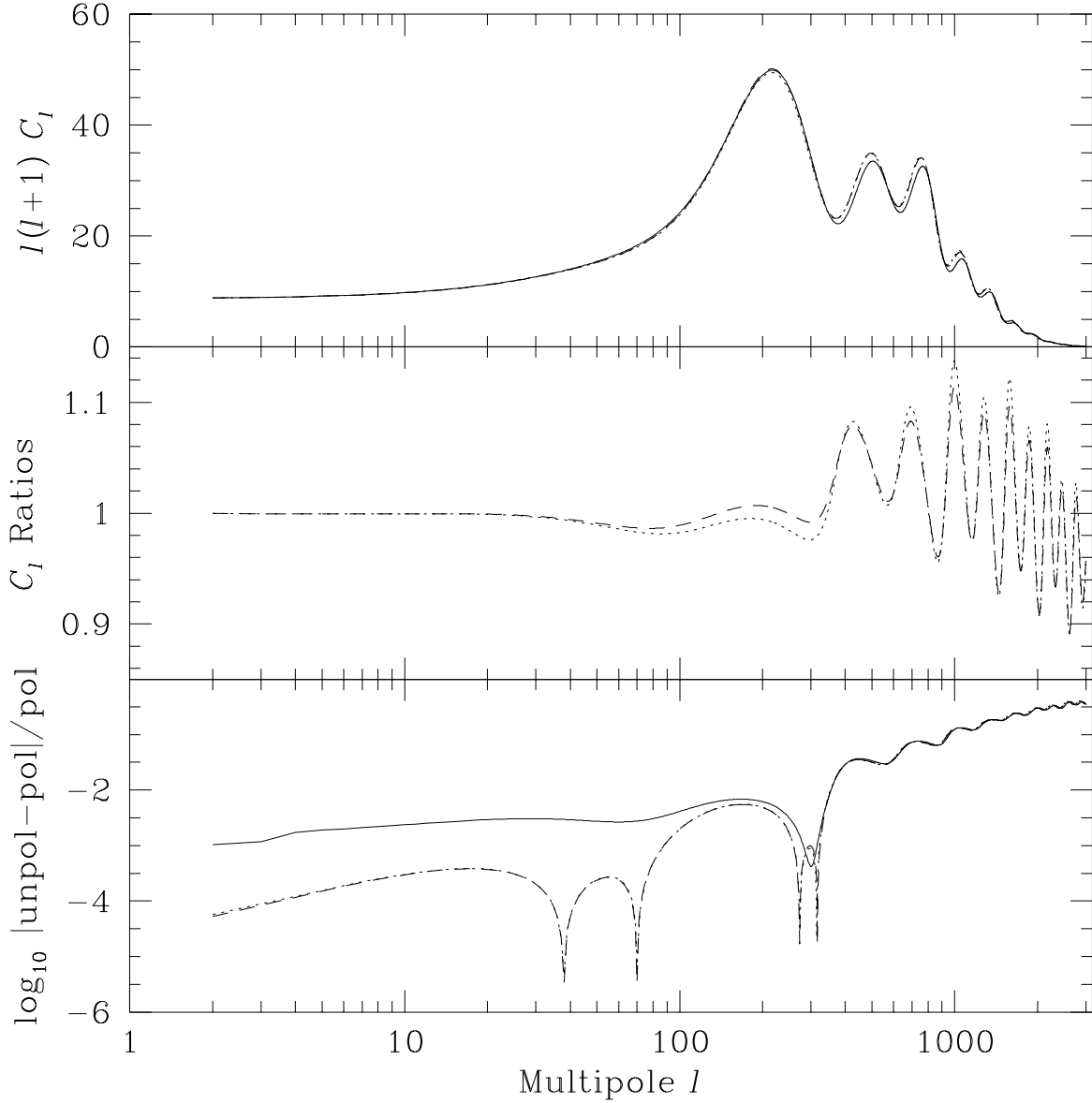


Fig. 1.— Top: The angular power spectrum C_l of the photon anisotropy (including polarization) in the CDM (solid), the $\Omega_\nu = 0.2$ CDM+HDM (dashed), and the $\Omega_\nu = 0.3$ CDM+HDM (dotted) models. Middle: The ratio of C_l for the CDM+HDM models relative to the CDM (dashed for $\Omega_\nu = 0.2$; dotted for $\Omega_\nu = 0.3$). Bottom: The fractional difference in C_l with and without polarization for the three models.

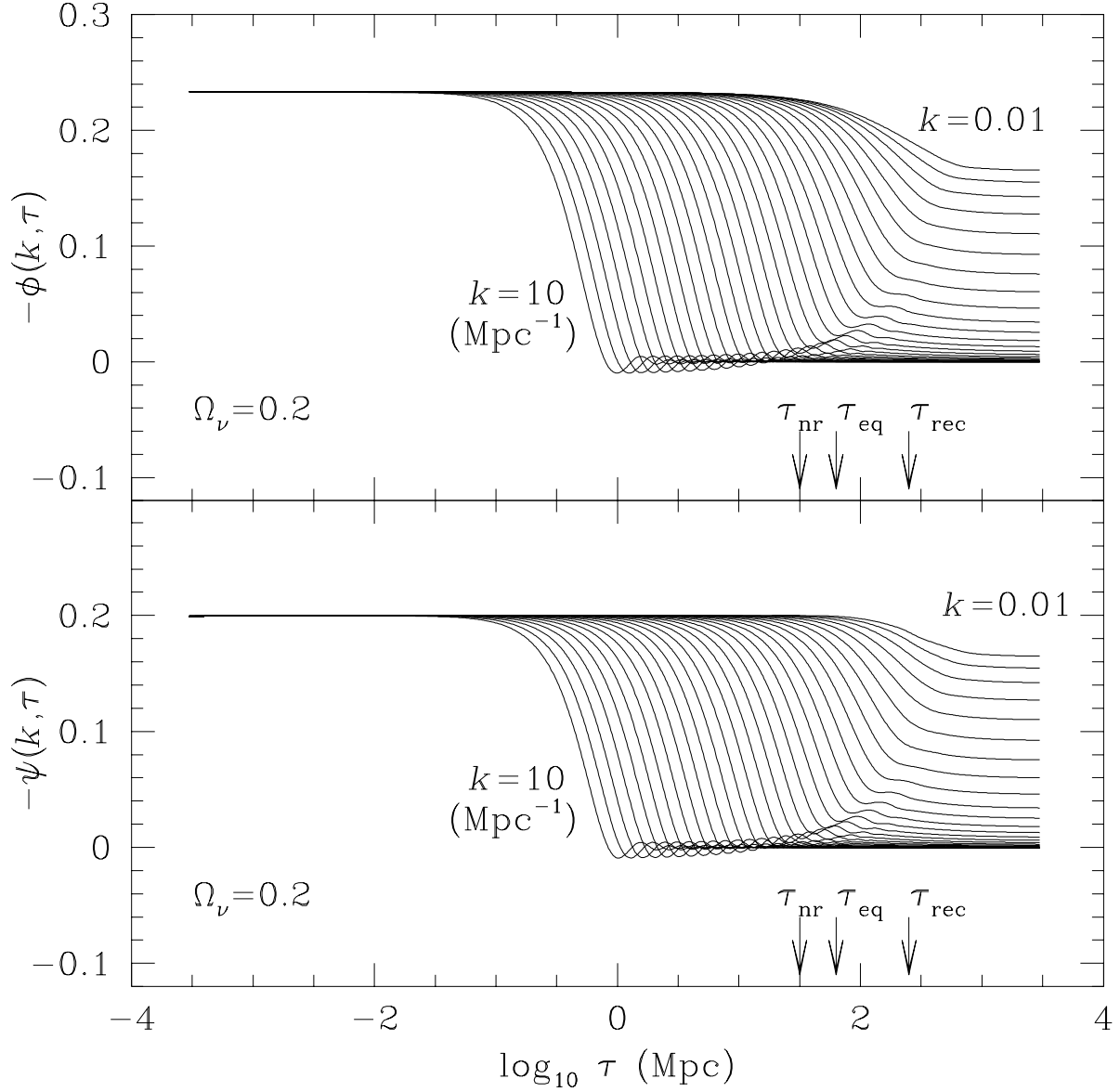
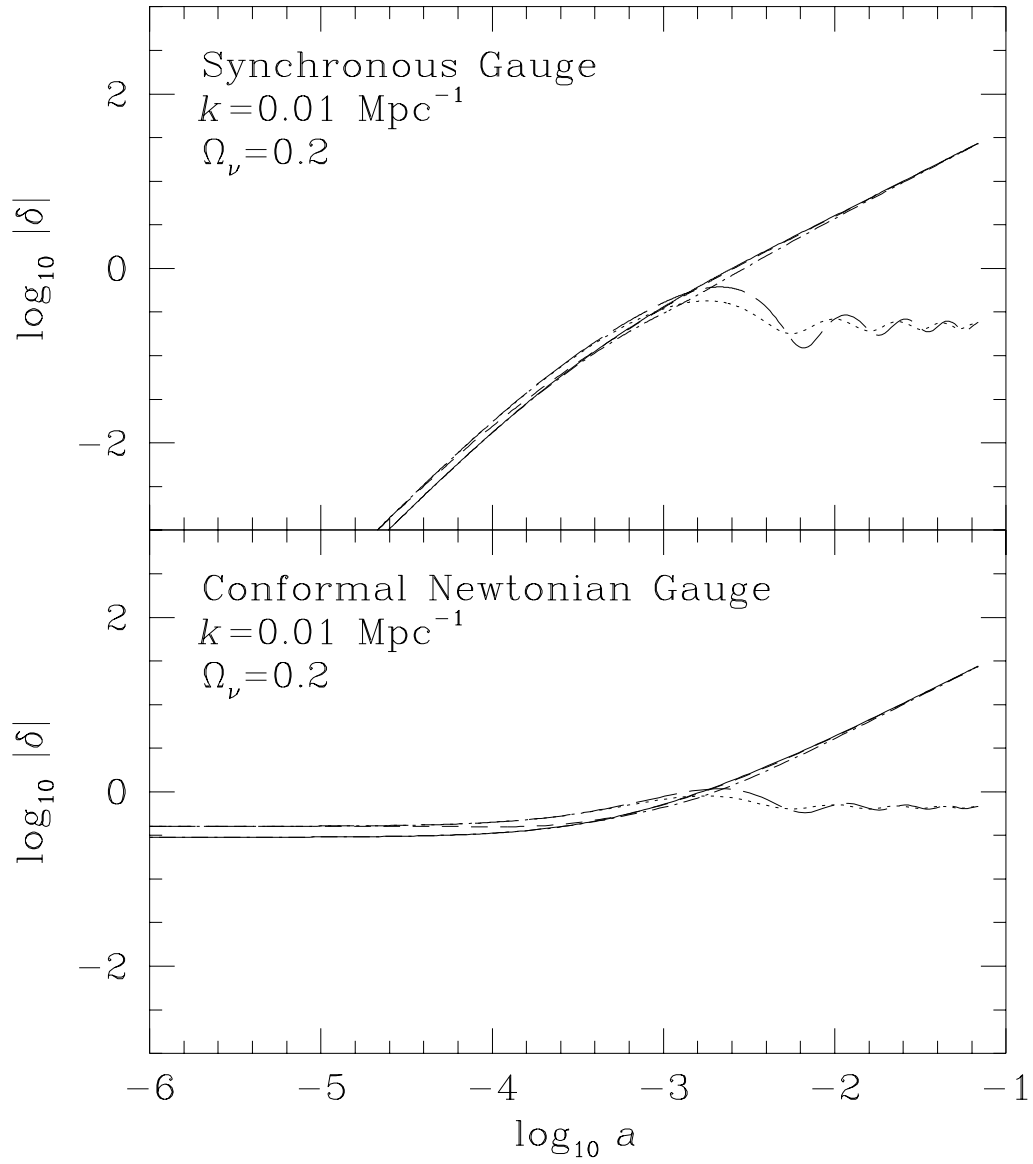
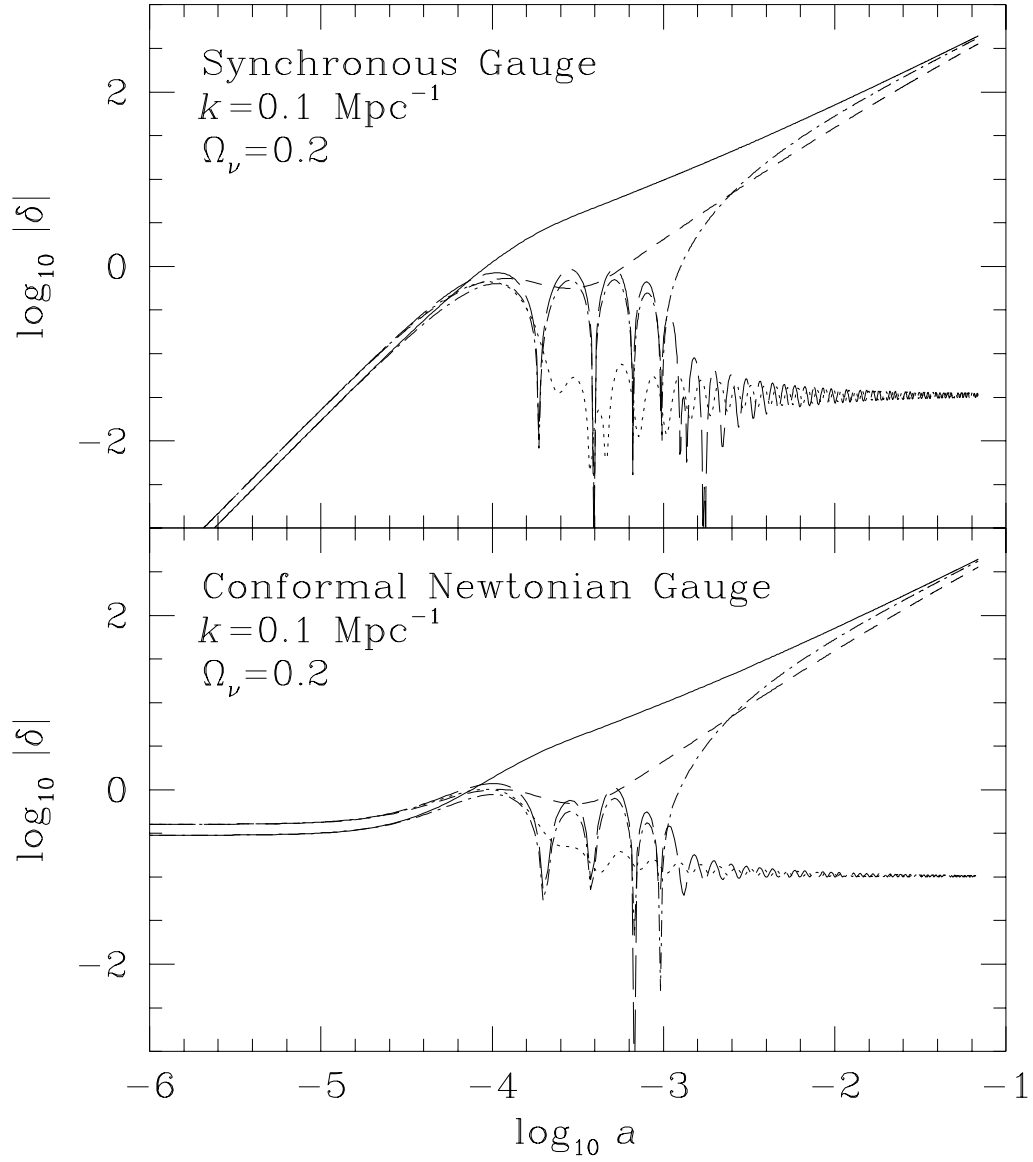


Fig. 2.— The scalar metric perturbations $\phi(k, \tau)$ and $\psi(k, \tau)$ in the conformal Newtonian gauge in the $\Omega_\nu = 0.2$ CDM+HDM model. The 31 curves from left to right correspond to 31 values of k between 10.0 Mpc^{-1} and 0.01 Mpc^{-1} . The labels τ_{nr} , τ_{eq} and τ_{rec} indicate, respectively, the time the 4.7 eV neutrinos become non-relativistic, the matter-radiation equality time, and the recombination time.





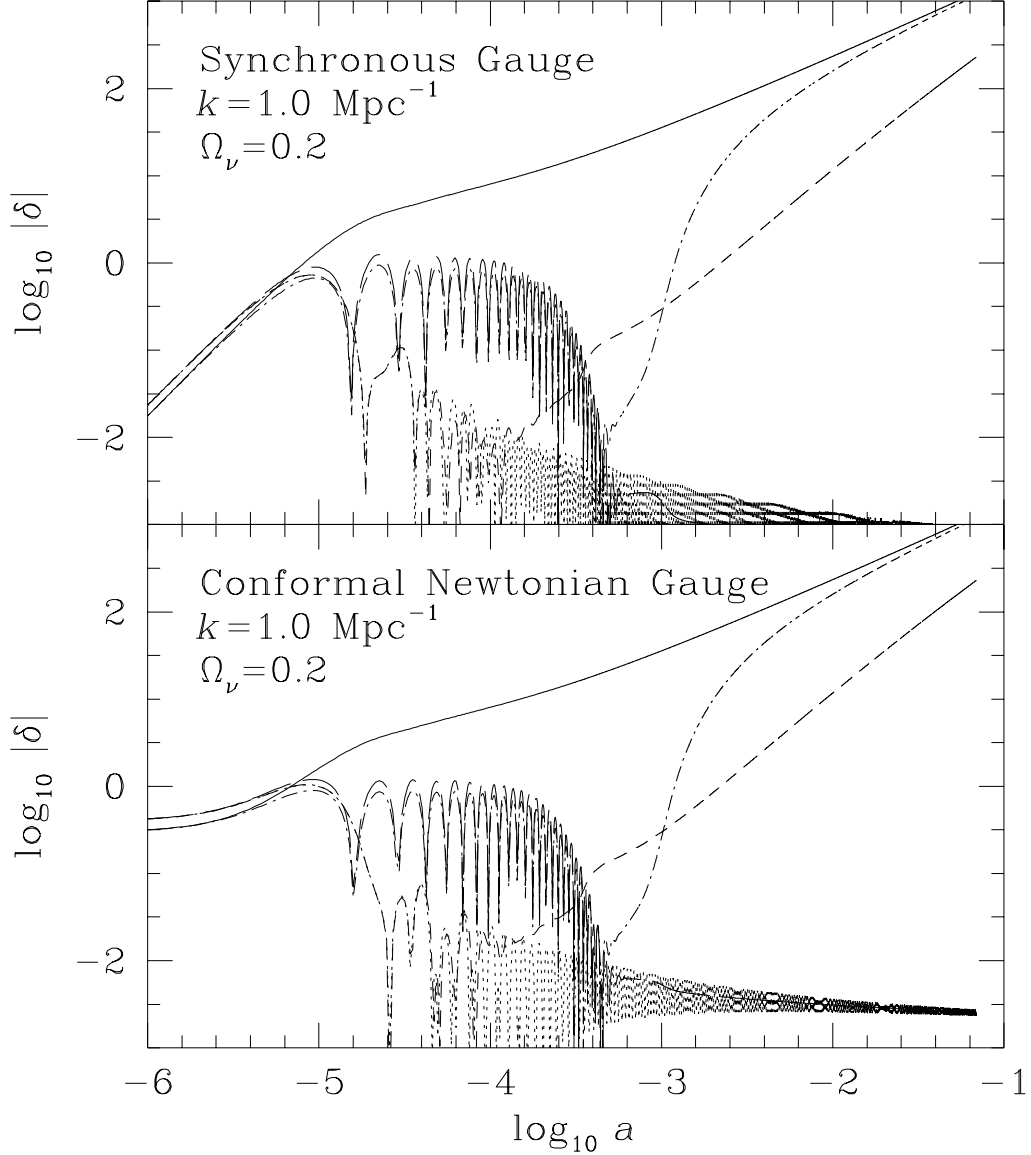


Fig. 3.— Evolution of the density fields in the synchronous gauge (top panels) and the conformal Newtonian gauge (bottom panels) in the $\Omega_\nu = 0.2$ CDM+HDM model for 3 wavenumbers $k = 0.01$ (Fig. 3a), 0.1 (Fig. 3b) and 1.0 (Fig. 3c) Mpc^{-1} . In each figure, the five lines represent $\delta_c, \delta_b, \delta_\gamma, \delta_\nu$ and δ_h for the CDM (solid), baryon (dash-dotted), photon (long-dashed), massless neutrino (dotted), and massive neutrino (short-dashed) components, respectively.

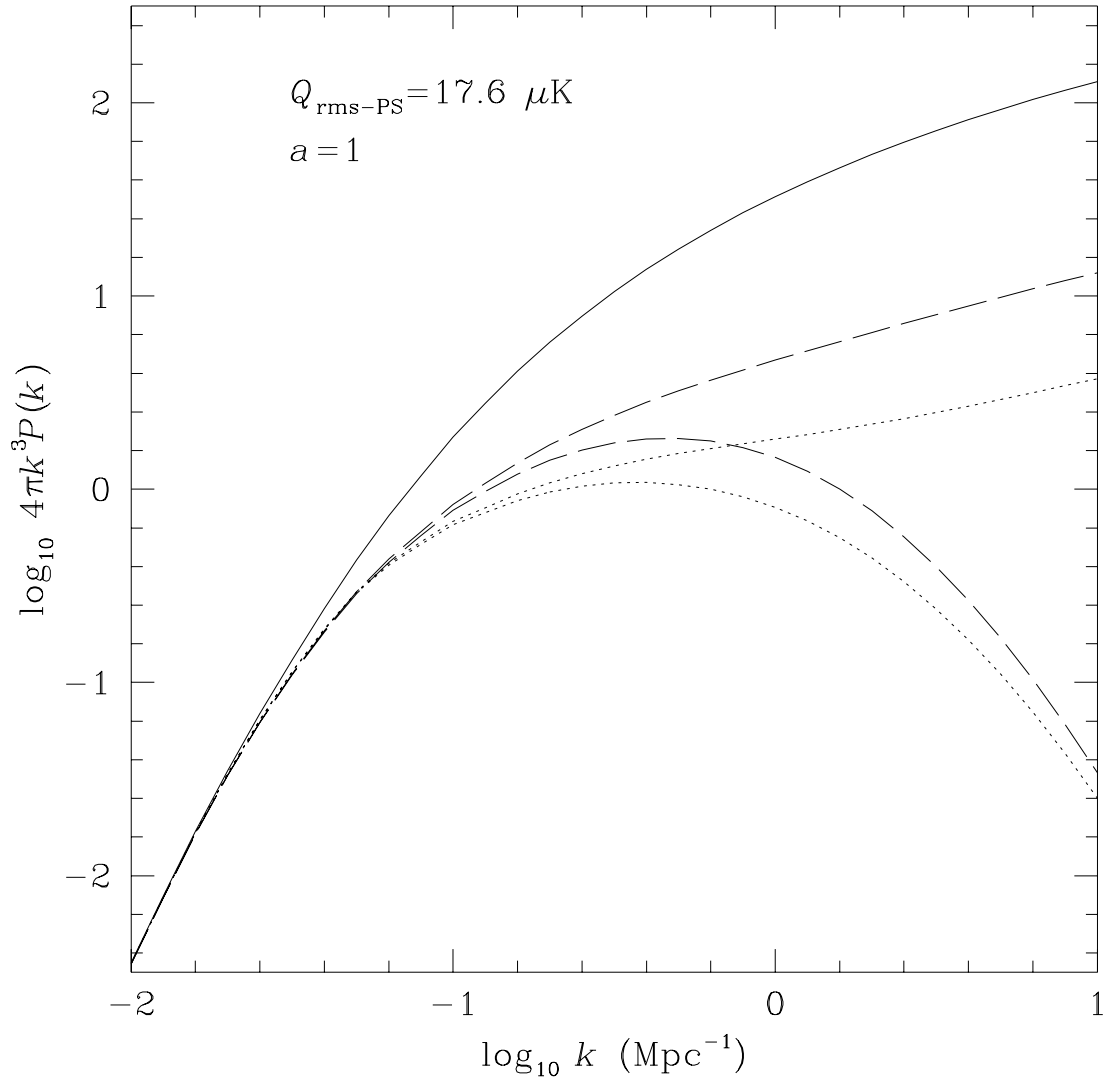


Fig. 4.— The $z = 0$ power spectra for the pure CDM (solid), the $\Omega_\nu = 0.2$ CDM+HDM (dashed), and the $\Omega_\nu = 0.3$ CDM+HDM (dotted) models. In the mixed models, the upper curve is for the CDM component and the lower one is for the HDM. The COBE-compatible quadrupole moment of $Q_{\text{rms-PS}} = 17.6 \mu K$ is used.